Stem Cell Reports
Article

ISSCR

OPEN ACCESS

Pluripotent stem cell derived dopaminergic subpopulations model the selective neuron degeneration in Parkinson's disease

Tony Oosterveen,[1,6] Pedro Garção,[1,6] Emma Moles-Garcia,[1,6] Clement Soleilhavoup,[1] Marco Travaglio,[1] Shahida Sheraz,[3] Rosa Peltrini,[1] Kieran Patrick,[1] Valerie Labas,[2] Lucie Combes-Soia,[2] Ulrika Marklund,[4] Peter Hohenstein,[3,5] and Lia Panman[1,*]

[1]MRC Toxicology Unit, University of Cambridge, Tennis Court Road, Cambridge CB2 1QR, UK
[2]PRC, INRA, CNRS, University of Tours, IFCE, Nouzilly, France
[3]Roslin Institute, University of Edinburgh, Edinburgh, UK
[4]Department of Medical Biochemistry and Biophysics, Karolinska Institute, Stockholm, Sweden
[5]Present address: Leiden University Medical Center, Leiden, the Netherlands
[6]These authors contributed equally
*Correspondence: liapanman1@gmail.com
https://doi.org/10.1016/j.stemcr.2021.09.014

SUMMARY

In Parkinson's disease (PD), substantia nigra (SN) dopaminergic (DA) neurons degenerate, while related ventral tegmental area (VTA) DA neurons remain relatively unaffected. Here, we present a methodology that directs the differentiation of mouse and human pluripotent stem cells toward either SN- or VTA-like DA lineage and models their distinct vulnerabilities. We show that the level of WNT activity is critical for the induction of the SN- and VTA-lineage transcription factors *Sox6* and *Otx2*, respectively. Both WNT signaling modulation and forced expression of these transcription factors can drive DA neurons toward the SN- or VTA-like fate. Importantly, the SN-like lineage enriched DA cultures recapitulate the selective sensitivity to mitochondrial toxins as observed in PD, while VTA-like neuron-enriched cultures are more resistant. Furthermore, a proteomics approach led to the identification of compounds that alter SN neuronal survival, demonstrating the utility of our strategy for disease modeling and drug discovery.

INTRODUCTION

Pluripotent stem cells (PSCs) are an important tool for disease modeling and drug-screening approaches. Several methodologies have been developed to generate neurons implicated in neurodegenerative disease such as dopaminergic, motor, and striatal projection neurons (Tao and Zhang, 2016). Substantia nigra (SN) dopaminergic neurons (DA) are highly susceptible to genetic and environmental toxicity, leading to their selective degeneration in Parkinson's disease (PD). In contrast, the related ventral tegmental area (VTA) DA neurons are more resistant to these insults (Surmeier et al., 2017). Access to PSC-derived cultures enriched for distinct DA subpopulations is an attractive approach to model the selective cell death of SN neurons in PD.

Midbrain DA (mDA) neurons are derived from midbrain floor-plate (FP) cells that are specified by Sonic Hedgehog (SHH), fibroblast growth factor 8 (FGF8), and WNT signaling during embryonic development (Smidt and Burbach, 2007). In several studies the timely addition of developmental relevant signaling molecules resulted in the efficient generation of functional mDA neurons from mouse and human PSCs (Kirkeby et al., 2012; Kriks et al., 2011; Lee et al., 2000; Nolbrant et al., 2017; Ying et al., 2003). These PSC-derived DA cultures are a mixture of neurons with both SN and VTA-like identities, but their relative contribution has not been analyzed in detail. Furthermore, subpopulation identity in these cultures was mainly based on late-onset markers that are not fully restricted to either the SN or VTA neuronal lineage (Fu et al., 2012; Reyes et al., 2012). In addition, the presence of other molecularly defined subpopulations of DA neurons (Poulin et al., 2020) has not been addressed in these cultures.

It is currently unclear how to generate DA cultures enriched for either SN or VTA neurons. The recent identification of SOX6 and OTX2 as early and selective markers of the SN and VTA neuronal lineages, respectively, demonstrated that DA subpopulation diversity is already established at neural progenitor stage, with SN neurons arising from medially located progenitors (Blaess et al., 2011; Panman et al., 2014; Poulin et al., 2014; Tiklova et al., 2019). WNT signaling plays an important role in the regulation of *Otx2* expression, which confers resistance to dopaminergic neurons and promotes VTA neuron differentiation (Di Salvio et al., 2010; Grealish et al., 2014; Prakash et al., 2006). Therefore, the early restricted expression of DA sublineage specific markers SOX6 and OTX2 suggests the requirement for optimized culture conditions that promotes the acquisition of either the SN- or VTA-specific neuronal lineage in PSC-derived progenitors.

Here we used insight from developmental studies to establish PSC differentiation conditions that promote the acquisition of SN-specific neuronal identities in mDA cultures. We show that temporal WNT signaling inhibition is required to induce medial FP precursors that are

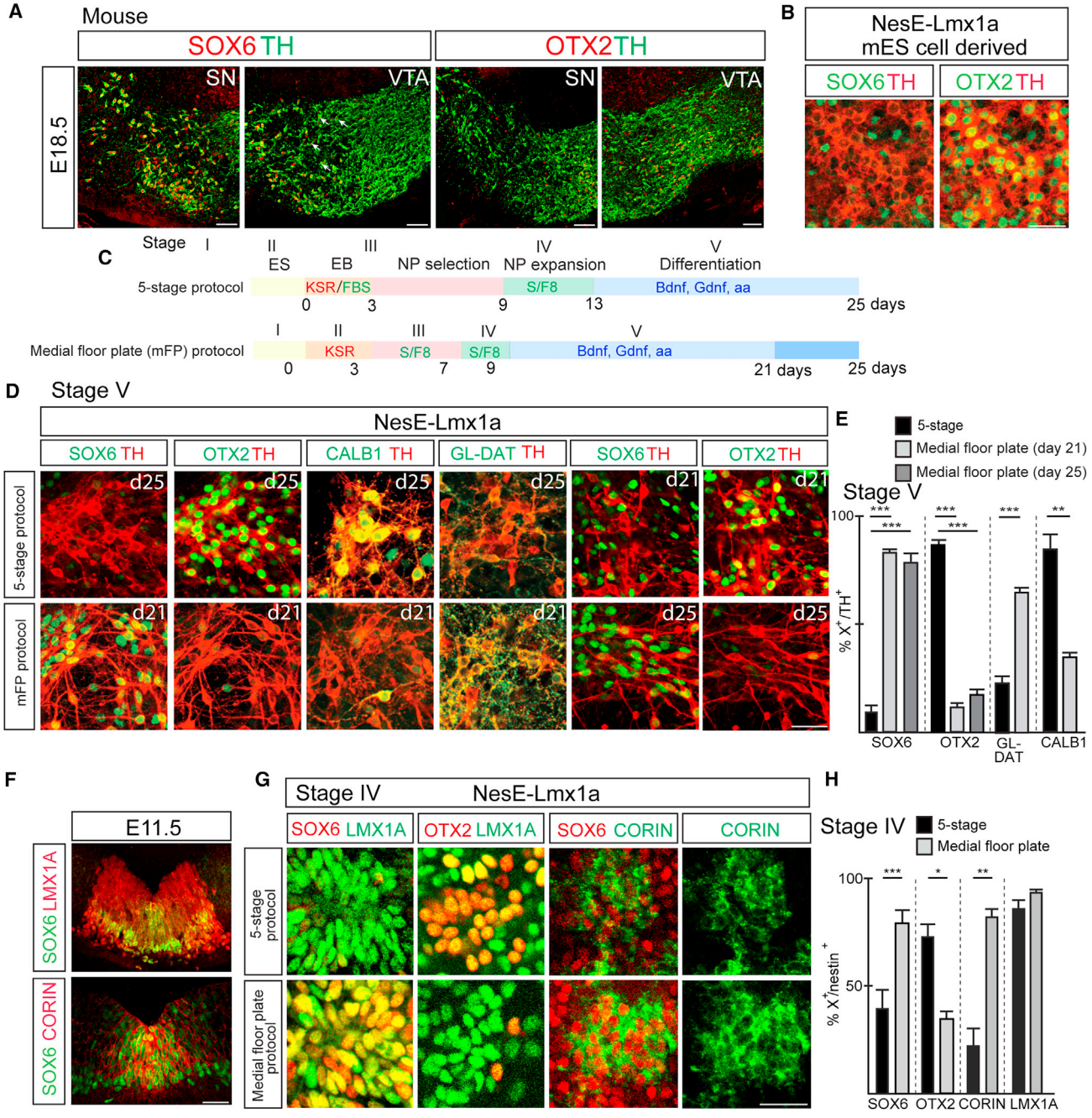

Figure 1. Directed differentiation of mESCs toward SN-like neuronal lineage

(A) Immunohistochemical (IHC) analysis of SOX6 and OTX2 in SN and VTA neurons of E18.5 mouse embryo. Arrows point to Sox6-expressing cells within VTA.

(B) IHC analysis of Nes-Lmx1a mESC-derived DA neurons.

(C) Schematic overview of the 5-stage and medial FP protocols.

(D) IHC analysis of NesE-Lmx1a ESC-derived neurons (stage V).

(E) Percentages of TH^+ neurons expressing the indicated neuronal markers in Nes-Lmx1a mESC-derived DA neurons (stage V). Mean values ± SD; one-way ANOVA with Bonferroni correction (SOX6 and OTX2) or unpaired t test (GlycoDAT and CALB1); n = 3 independent experiments.

(F) IHC analysis of midbrain FP of E11.5 mouse embryo.

(legend continued on next page)

efficiently directed toward the SN-like neuronal lineage. Furthermore, we demonstrate that our strategy enables the derivation of distinct DA subpopulations that are distinguishable by their selective sensitivity to mitochondrial toxicity, providing a tool to model PD *in vitro*.

RESULTS

Directing differentiation of mESC-derived medial FP precursors toward SN-like neuronal lineage

SOX6 and OTX2 are early and selective DA sublineage determinants during mouse embryonic development (Panman et al., 2014) (Figures 1A and 1F). While OTX2 is solely confined to VTA neurons, SOX6 is expressed in SN neurons, the parabrachial pigmented (PBP) part of the VTA, and the retrorubral field (RRF) (Figure 1A; Poulin et al., 2020). To investigate the early aspects of SN and VTA neuronal lineage specification during PSC differentiation, we assessed the percentage of SOX6- and OTX2-labeled DA neurons derived from wild-type and NesE-Lmx1a mouse embryonic stem cells (mESCs) (Friling et al., 2009; Panman et al., 2011) differentiated according to the 5-stage protocol as previously described (Lee et al., 2000) (Figure 1C and Table S1, protocol 3). Remarkably, only a small proportion (less than 10%) of DA neurons derived from wild-type or NesE-Lmx1a (Figures 1B, S1A, S1B, and S1F) ESC lines expressed SOX6, while the majority of the neurons (more than 80%) were OTX2 positive (Figures 1B, S1A, S1B, and S1F). Consistently, a large fraction of the neurons was positively labeled for CALBINDIN1 (CALB1) and negatively for GlycoDAT (Figure S1F), indicating that most neurons have VTA-like identities. The distinct spatial-temporal origin of DA subpopulations (Blaess et al., 2011; Panman et al., 2014) suggests that different culture conditions may be needed for inducing the SN neuronal lineage. Therefore, we decided to systematically alter several steps of the 5-stage protocol to define SN neuronal lineage-promoting conditions (see Table S1 for a summary). We replaced fetal bovine serum with knockout serum replacement (KSR) during the embryonic body (EB) formation (stage II; Figure 1C and Table S1, protocol 1), which did not alter the differentiation outcome of the 5-stage protocol, with the majority of neurons expressing VTA-specific markers (Figures 1D and 1E). However, when using KSR in combination with earlier and shorter exposure of progenitors at the neural progenitor (NP) selection stage (stage III) and NP expansion stage (stage IV) to SHH and FGF8 (S/F8), nearly all NesE-Lmx1a mESC-derived DA neurons became SOX6 positive (83%) and there was a striking reduction in the number of OTX2-labeled DA neurons (12%) (Figures 1C–1E and Table S1, protocol 2). We termed this modified version the "medial FP (mFP) protocol," referring to the developmental origin of SN neurons. Similar results were obtained when using wild-type ESCs or a second independently generated NesE-Lmx1a ESC line (Figures S1A and S1B). Extending the mFP protocol to 25 days did not result in an increase of OTX2-expressing neurons (Figures 1D and 1E). The specification of SN-like specific neuronal identities under the mFP protocol was further supported by the increase in GLYCODAT-labeled (from 23% to 65%) and decrease in CALB1-labeled (from 85% to 34%) DA neurons (Figures 1D and 1E). In addition, Sox6-expressing neurons were positive for ALDH1A1 (Figure S1D), further supporting the SN-like neuronal identity. The altered culture conditions did not compromise DA cell numbers (35% TH/4′,6-diamidino-2-phenylindole [DAPI] in both 5-stage and mFP protocol) and midbrain identity as revealed by the maintenance of FOXA2, LMX1A, NR4A2, and EN1 expression (Figures S1A and S1C). Remarkably, the use of KSR during EB formation in combination with the addition of the growth factors S/F8 during the NP selection stage for 4 days (stage III) and NP expansion stage for 2 days (stage IV) are essential protocol steps for promoting SN-like subpopulation identity (Figure 1C and Table S1, protocol 2), and any variation on this protocol abolished the production of healthy-looking Sox6-expressing DA neurons (Figures S1E–S1G and Table S1).

In the medial part of the FP, SOX6-labeled cells coexpress CORIN (Figure 1F). Next, we investigated whether mFP cells are initially specified when using SN neuron-promoting culture conditions. Indeed, we observed a robust increase in SOX6-labeled (90%) and CORIN-labeled (82%) DA progenitor cells at stage IV of the mFP protocol, while the 5-stage-protocol mainly yielded the lateral OTX2-expressing DA progenitors (Figures 1G and 1H). The unaltered expression of LMX1A shows that DA progenitors are generated with similar efficiency in both protocols (Figure 1H).

Canonical WNT signaling mediates dopaminergic subpopulation diversification

By altering the timing of growth factor exposure during mESC differentiation, we were able to switch dopaminergic subpopulation identity of the obtained cultures from VTA- to SN-like. A possible explanation for this lineage switch is

(G) IHC analysis of DA progenitor markers in Nes-Lmx1a mESC-derived progenitors (stage IV).
(H) Percentage of NESTIN$^+$ cells expressing indicated markers in Nes-Lmx1a mESC-derived neural progenitors (stage IV). n = 3 independent experiments; mean values ± SD; unpaired t test.
*p < 0.05, **p < 0.01, ***p < 0.001. Scale bars, 100 μm (A and F) and 50 μm (B, D, and G).

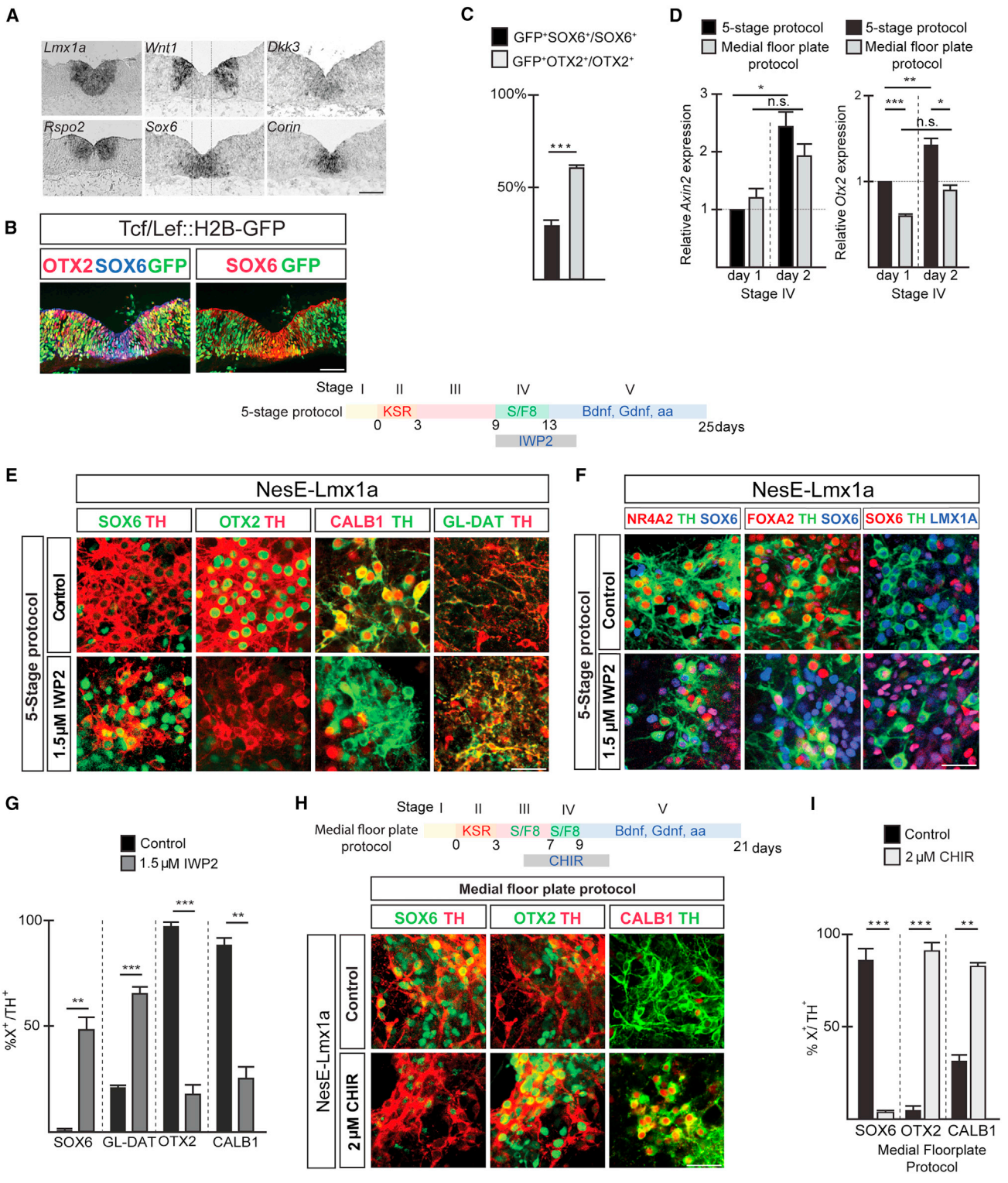

Figure 2. Differential WNT signaling levels regulate DA neuronal subpopulation specification during mESC differentiation

(A) Gene expression patterns of WNT signaling components in relation to *Sox6* and *Lmx1a* in the FP of E11.5 mouse embryo.

(B) IHC analysis of the midbrain FP of Tcf/Lef::H2B-GFP reporter mouse line at E11.5. Reporter activation is visualized by GFP expression.

(legend continued on next page)

the protocol-dependent differential production of endogenous canonical WNT signaling. Expression analysis demonstrates that the WNT/β-CATENIN signaling pathway is selectively activated in OTX2$^+$ lateral dopaminergic progenitors as shown by the lateral localization of *Wnt1* and *Rspo2* transcripts, the medial expression of repressors *Dkk1* (Ribeiro et al., 2011) and *Dkk3* (Nakamura and Hackam, 2010) (Figure 2A), and overlap between GFP-labeled WNT responding progenitor cells with OTX2 in the Tcf/Lef::H2B-GFP reporter mouse line. Furthermore, canonical WNT target genes *Axin2* (Jho et al., 2002) and *Otx2* (Chung et al., 2009) are higher expressed in 5-stage than in mFP-protocol-derived progenitors at days 1 and 2 of stage IV of the respective protocols (Figure 2D), indicating that production of WNT signaling could indeed be culture condition dependent. Next, we tested whether addition of canonical WNT inhibitors or activators to differentiating progenitors promotes the acquisition of SN- or VTA-like identities in dopaminergic cultures, respectively. Neural progenitors displayed expected responsiveness to WNT activator CHIR (Ying et al., 2008) and inhibitors IWP2 and IWR1 (Chen et al., 2009) as observed by up- or downregulation of *Axin2*, respectively (Figures S1H–S1J). Five-stage protocol-derived progenitors (Figure 2E) treated for 6 days with WNT inhibitor IWP2 showed an increased percentage of SOX6- and GLYCO-DAT-labeled dopaminergic neurons and reciprocally a drastic downregulation of VTA restricted markers OTX2 and CALB1 (Figures 2E and 2G). While the selected timing and duration of IWP2 treatment had only a minor effect on dopaminergic cell numbers (32% TH/DAPI), mDA identity was preserved as shown by overlap of SOX6 with NR4A2, FOXA2, and LMX1A expression (Figure 2F). To assess whether Wnt signaling activation is sufficient to control SN- to VTA-like neuronal lineage conversion, we treated mFP-derived progenitors for 6 days with CHIR during stage III and IV (Figure 2H). This resulted in a robust decrease of SOX6- and an increase of OTX2- and CALB1-labeled dopaminergic neurons (Figures 2H and 2I), indicating that WNT activation promotes VTA neuronal lineage specification. The WNT-mediated dopaminergic lineage switch already takes place at progenitor stage, as WNT activation and inhibition resulted in down- and upregulation, respectively of medial progenitor markers *Corin* and *Sox6* (Figure S1K).

Mitochondrial toxin exposure results in the selective degeneration of SN neurons (Bove et al., 2005). To test whether we can recapitulate the selective vulnerability of DA neurons *in vitro*, we compared the effects of mitochondrial toxins on neuronal survival between 5-stage and mFP-derived cultures (Figure 3A). The mFP protocol-derived DA cultures displayed increased sensitivity to mitochondrial toxins with a strong increase in the number of apoptotic neurons as visualized by cCASP3 labeling (Figures 3F and 3I) and a decrease in number of TH-expressing cells (Figures 3C and 3D) after treatment with MPP$^+$ and rotenone for 48 h. In contrast, 5-stage protocol-derived DA neurons were significantly less affected by these mitochondrial toxins (Figures 3B, 3D, 3E, and 3I). To address whether there is a direct correlation between the presence of SOX6-labeled DA neurons in cultures and increased vulnerability, we analyzed the effects of mitochondrial toxins on cell survival after manipulating SOX6 levels by Wnt signaling modulators. No effects on cell death and TH$^+$ cell numbers were observed after addition of Wnt signaling inhibitors and activators to differentiating cultures without toxin exposure (Figures 3A–3I). However, the IWP2-mediated induction of SOX6 in 5-stage protocol-derived cultures rendered these neurons far more sensitive to MPP$^+$ and rotenone, resulting in reduction of TH-labeled cells (Figures 3B and 3D) and an increase in cCASP3 expression (Figures 3E and 3I). Interestingly, reducing SOX6 expression in mFP-derived cultures by CHIR exposure (Figure 2G) reversed the effects of mitochondrial toxins on cell survival (Figures 3C, 3D, 3F, and 3I). Consistent with the increased sensitivity of SOX6-enriched DA cultures, cCASP3 expression was mainly induced in SOX6-labeled DA neurons while OTX2 DA neurons were largely unaffected (Figures 3G, 3H, 3J, and 3K). Altogether, differential levels of Wnt signaling directs DA sublineage selection and consequently determines the vulnerability of obtained cultures.

(C) Percentage GFP$^+$ DA neuronal progenitors expressing either SOX6 or OTX2 in the Tcf/Lef::H2B-GFP reporter mouse line. Mean values ± SD; unpaired t test; n = 3 independent experiments.

(D) qPCR analysis of *Axin2* and *Otx2* expression levels in NesE-Lmx1a ESC-derived neural progenitors at day 1 and day 2 of stage IV. n = 5 independent experiments; mean values ± SEM; two-way ANOVA with Bonferroni correction; n.s., not significant.

(E) Experimental design differentiation protocol. IHC analysis of NesE-Lmx1a ESC DA cultures (stage V).

(F) DA marker analysis of NesE-Lmx1a mESC-derived cultures differentiated according the 5-stage protocol (stage V) and treated with 1.5 μM IWP2.

(G) Percentages of TH$^+$ neurons expressing the indicated markers in NesE-Lmx1a ESC-derived cultures (stage V) differentiated as described in (E). Mean values ± SD; unpaired t test; n = 3 independent experiments.

(H) Scheme of differentiation protocol. Immunohistochemical analysis of control and CHIR-treated cultures (stage V).

(I) Percentages of TH$^+$ neurons expressing indicated markers differentiated as described in (H). Mean values ± SD; unpaired t test; n = 3 independent experiments.

*$p < 0.05$, **$p < 0.01$, ***$p < 0.001$. Scale bars, 50 μm.

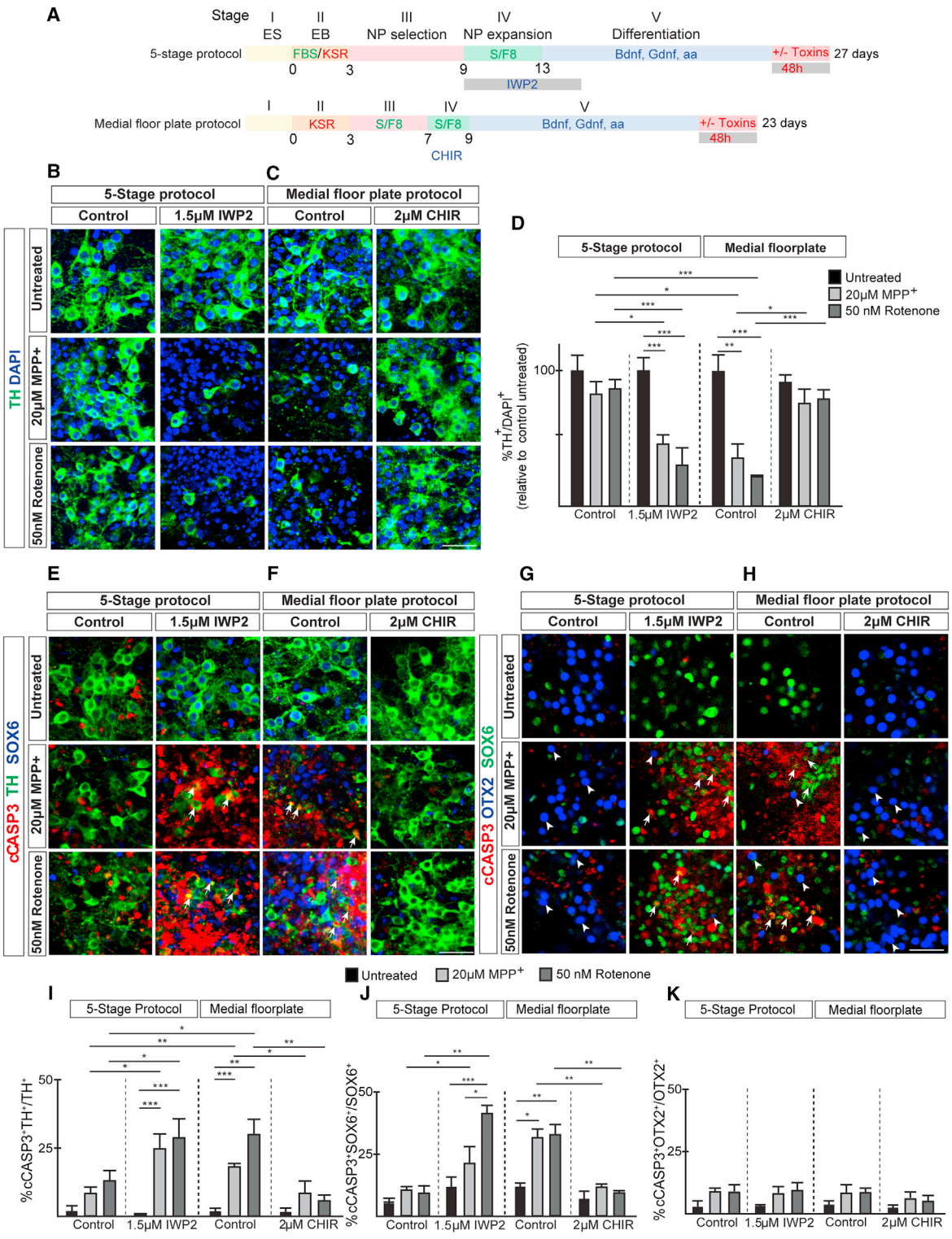

Figure 3. Modulation of WNT signaling affects the sensitivity of neurons to mitochondrial toxins

(A) Diagram presenting the mESC differentiation conditions.

(B and C) (B) Analysis of TH in relation to DAPI in cultures differentiated according the 5-stage protocol and (C) the medial FP protocol.

(legend continued on next page)

WNT signaling inhibition directs hESC differentiation toward SN-like DA neuronal lineage

In the human fetal brain, SOX6 is expressed in SN neurons (93%) (Figures 4A and 4B), the PBP part of the VTA (Figure 6A), and the RRF (data not shown), while OTX2 is mainly confined to the VTA (Figures 4A, 4B, and 6A) except for a few labeled cells in the SN (5%). Human ESC (hESC)-derived DA neurons differentiated according to a modified version of the FP protocol (Kriks et al., 2011) were mainly expressing OTX2 and were negative for SOX6 (Figure 4C). We first addressed whether human DA progenitors, defined by LMX1A expression (Marklund et al., 2014), could be subdivided into distinct domains, analogous to the mouse. *SOX6*- and *CORIN*-labeled cells are confined to the medial progenitor domain in the CS16 human embryonic midbrain (Figure 4E). The laterally defined expression of *WNT1* (Figure 4E) suggests a role for WNT/β-CATENIN signaling in DA subpopulation specification and prompted us to investigate whether WNT inhibition promotes SN-like lineage specification also during hESC differentiation.

SHH and WNT are inducers of LMX1A and OTX2 expression, which through feedforward mechanisms enhance WNT signaling (Chung et al., 2009; Prakash et al., 2006), possibly resulting in VTA neuronal lineage-inducing culture conditions. Therefore, we decided to test the potential of IWP2 to induce SN-specific lineage markers in cultures that were exposed to different levels of SHH pathway activation and altered durations of WNT signaling, as illustrated in Figures S2A and S2F. SHH pathway activation was lowered by using Smoothened Agonist (SAG) (Figure S2F), as confirmed by reduced *GLI1* expression (Figure S3D). The window of CHIR exposure was shortened from days 4–13 to days 4–11 (referred to as CHIR and control condition, respectively; Figures 4D, S2A, and S2F), lowering the levels of canonical WNT target genes *AXIN2* and *SP5* (Figure S3E). The use of SAG and/or removal of CHIR at day 11 did not affect general aspects of DA neuron specification, with high percentages (about 75%) of LMX1A$^+$FOXA2$^+$ double-labeled progenitors (Figures S2D, S3A, and S3F) and LMX1A-, FOXA2-, and NR4A2-positive DA neurons observed (Figures S2E, S4A–S4C, and S4I). IWP2 was added to the cultures at or after day 11 to prevent interference with DA neuron generation in general (Figures S2A and S2F). Testing several culturing conditions (as outlined in Figures S2A and S2F), we concluded that exposure of SAG-treated control DA progenitors to 0.5 and 1 μM IWP2 between day 11 and day 16 resulted in the most robust induction of SOX6 in DA neurons (Figure S2G). Any other variation in timing and concentration of IWP2 addition resulted in less optimal outcomes (Figures S2F and S2G). Moreover, the addition of IWP2 (0.5–4 μM from day 11 to day 16/18) to DA progenitors treated with high-dose SHH did not result in the induction of any SOX6-labeled DA neurons and there was no decrease of OTX2 expression (Figures S2A, S2B, and S2D), suggesting that under these conditions progenitors lack the competence to acquire SN-like lineage characteristics in response to WNT inhibition.

Exposure of SAG-treated control DA progenitors to 0.5 and 1 μM IWP2 at days 11–16 (Figure 4D) significantly increased the percentage of SOX6-labeled DA neurons (39% with 1 μM IWP2) compared with CHIR (7%) and control (12%) conditions after 25 days. Reciprocally, the number of OTX2$^+$ DA neurons significantly decreased under the same conditions (CHIR: 65%; control: 53%; 1 μM IWP2: 28%) (Figures 4F, 4G, S2F, and S2G). SOX6 and OTX2 expression did not overlap in DA neurons from IWP2-treated cultures (Figure 4F). Similar results were obtained with WNT antagonist DKK1 (Figure 4G). In addition, DA subpopulation-specific markers KCNJ6 (GIRK2) (Figures S4D and S4E) and CALB1 (Figure S4F) were up- and down-regulated, respectively, by IWP2 treatment (Figures S4J and S4K), consistent with acquisition of SN-like identities. The IWP2-induced SOX6-positive DA neurons coexpressed SATB1 (Figure S4G) and ALDH1A1 (Figure S4H) (Anderegg et al., 2015), further confirming their SN-specific identity. Furthermore, the use of SAG in combination with IWP2 did not compromise midbrain identity, with most progenitors LMX1A$^+$FOXA2$^+$ double positive (Figure S3A) and more than 70% of DA neurons coexpressing LMX1A, NR4A2, and FOXA2 under all conditions (Figures S4A, S4B, S4C, and S4I). IWP2-mediated induction of SOX6$^+$ SN-like DA neurons was reproduced in an independent human induced PLC (iPSC) line carrying a triplication of the

(D) Graph showing the percentage of TH-expressing neurons in relation to DAPI. Mean values ± SD; two-way ANOVA with Bonferroni correction; n = 3 independent experiments.

(E and F) (E) IHC analysis of cultures differentiated according the 5-stage protocol and (F) the medial FP protocol. Arrows point to cCASP3$^+$ TH$^+$-labeled neurons.

(G and H) (G) IHC analysis of cultures differentiated according the 5-stage protocol and (H) the medial FP protocol. Arrows point to cCASP3$^+$ SOX6$^+$-labeled neurons. Arrowheads indicate OTX2$^+$ neurons negatively labeled for cCASP3.

(I–K) Graphs showing (I) the percentage of cCASP3 in relation to TH, (J) the percentage cCASP3-expressing cells in relation to SOX6, and (K) the percentage cCASP3-expressing cells in relation to OTX2 under various culture conditions. Mean values ± SD; two-way ANOVA with Bonferroni correction; n = 3 independent experiments.

*p < 0.05, **p < 0.01, ***p < 0.001. Scale bars, 50 μm.

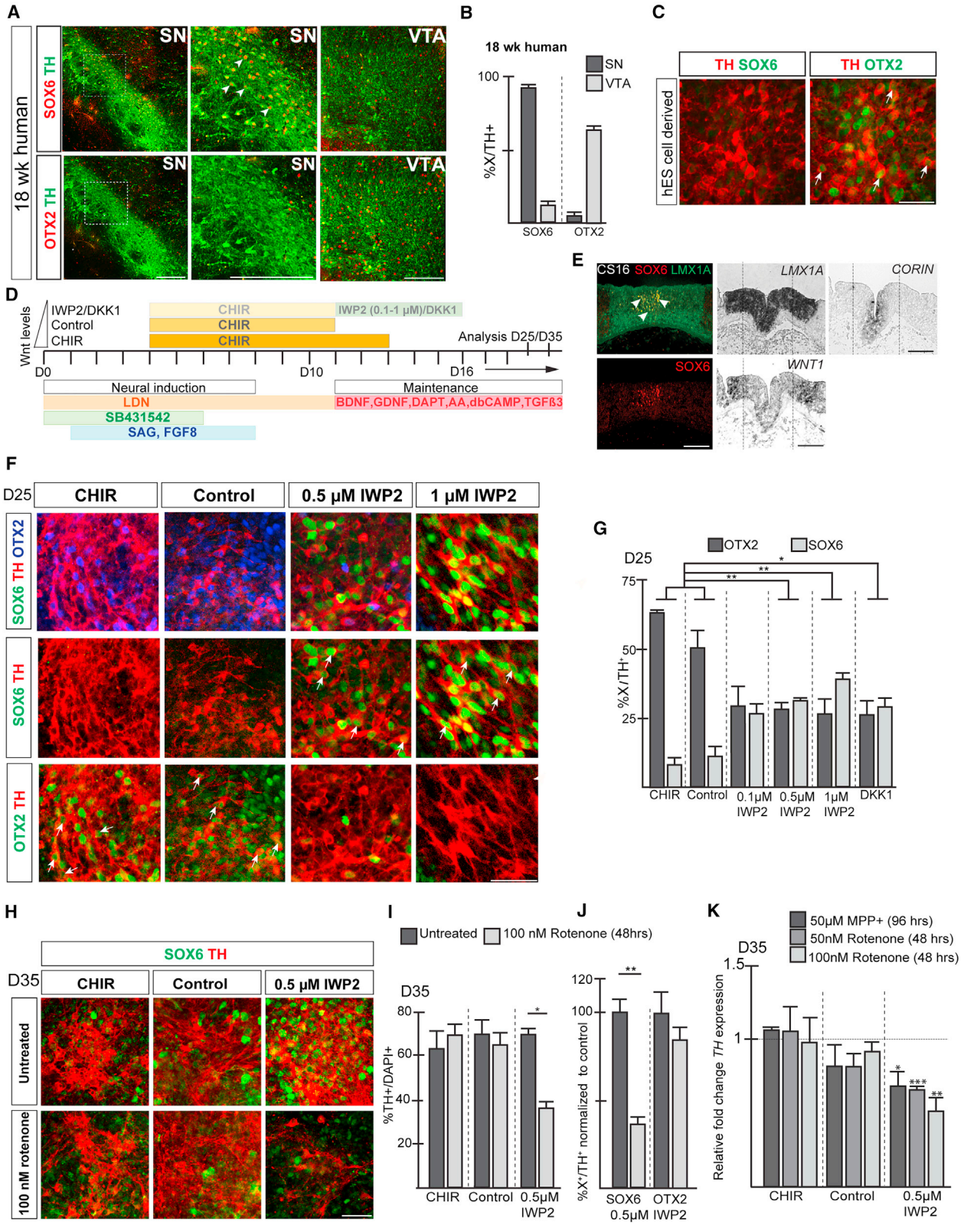

(legend on next page)

α-synuclein locus (AST) (Devine et al., 2011) (Figures S5A–S5C).

To address whether DA sublineage selection takes place at a progenitor level in human cultures, we analyzed the effect of WNT signaling modulation in DA progenitors. As expected, IWP2 treatment resulted in a downregulation of *AXIN2* and *SP5* expression at day 13 compared with control conditions, while increased levels were observed under CHIR conditions (Figure S3E). *OTX2* and *SOX6* were down- and upregulated, respectively, in DA progenitors upon IWP2 treatment (Figures S3B and S3F), consistent with the sublineage selection. While SOX6 and OTX2 were overlapping in control and CHIR-treated cultures, their expression became separate in IWP2 culture conditions. The IWP2-dependent increase of *CORIN* expression (Figures S3C and S3G) further demonstrates that the induction of medial progenitor markers correlates with the acquisition of the SN-like neuronal lineage also during human embryonic development.

We predicted that IWP2-mediated induction of SOX6 would also confer sensitivity to toxic insult. While there was only a minor effect of rotenone and MPP^+ in CHIR and control cultures, there was a very strong reduction in DA neurons in cultures differentiated in the presence of IWP2 (Figures 4H–4K). In particular, there was a loss of SOX6-positive DA neurons while OTX2-expressing neurons remained unaffected (Figure 4J), further demonstrating the selective sensitivity of $SOX6^+$ DA neurons to toxic insults. In agreement with the lack of Sox6 induction, IWP2 treatment did not confer sensitivity to mitochondrial toxicity in DA neurons differentiated in the presence of SHH-C24II + Pur (Figure S2C). Altogether, we demonstrate that by modulating WNT signaling levels during human PSC differentiation, we acquire distinct DA subpopulations that display selective sensitivity to mitochondrial toxins according to their identity.

Forced expression of Sox6 induces SN-like identities in human PSC-derived DA cultures

Previously, we have shown that efficient neuronal lineage induction under non-permissive culturing conditions can be achieved by overexpression of transcriptional determinants in PSC-derived progenitors (Friling et al., 2009; Panman et al., 2011). Therefore, we decided to test whether forced expression of SOX6 can induce SN neuron-specific markers also when cultures are exposed to high levels of SHH signaling. As described previously, DA neurons differentiated according to the FP protocol (Kriks et al., 2011) (Figure 5B) were mainly negative for SOX6 at day 35 (Figures 4B, 5C, and 5F), while VTA-specific markers OTX2 and CALB1 were more abundantly represented (Figures 4B, 5C, 5D, and 5F). Although SOX6 is only expressed in a small population of DA progenitors (Figures 4D [CS16] and 5A [CS20]), its expression is strongly induced in early post-mitotic neurons in a region complementary to OTX2 (Figure 5A). Consistent with these expression patterns, we transduced early post-mitotic cultures with lentiviral expression vectors for SOX6 (L-SOX6) and OTX2 (L-OTX2) at day 20 and analyzed their ability to induce DA subpopulation-specific expression at day 35 (Figure 5B). High percentages of SOX6-expressing (79%) and OTX2-expressing (75%) DA neurons were obtained upon lentiviral transduction (Figures 5C and 5F). Analysis of L-SOX6 transduced cultures revealed that a large proportion of DA neurons expressed GIRK2 (73% versus 30% in controls) (Figures 5E and 5F) and were negatively labeled for OTX2

Figure 4. WNT inhibition induces SOX6 in hESC-derived DA neurons and confers sensitivity to mitochondrial toxins

(A) IHC analysis of the human fetal brain.

(B) Percentage of SN and VTA DA neurons expressing either SOX6 or OTX2 in the human fetal midbrain.

(C) Expression of SOX6 and OTX2 in hESC-derived TH-positive neurons.

(D) Schematic overview depicting hESC differentiation conditions. CHIR (CHIR from day 4 to day 13), control (CHIR from day 4 to day 11), and IWP2 (IWP2 from day 11 until day 16).

(E) Analysis of FP markers in human embryo (cs16). Arrowheads indicate overlap of SOX6 and LMX1A expression. Dashed lines indicate medial/lateral division within progenitor domain.

(F) IHC analysis of hESC-derived cultures (day 25). Arrows point to $OTX2^+/TH^+$-labeled neurons in CHIR and control cultures and $SOX6^+/TH^+$-labeled neurons in IWP2-treated cultures. Differentiation conditions as described in (D).

(G) Percentage of TH^+ neurons expressing SOX6 or OTX2 differentiated as described in (D). Mean values ± SD; one-way ANOVA with Bonferroni correction; n = 4 independent experiments.

(H) Analysis of SOX6 and TH expression in hESC-derived cultures treated with rotenone for 48 h at day 35.

(I) Percentage of TH^+ neurons after treatment with either dimethyl sulfoxide (DMSO) or rotenone for 48 h at day 35 differentiated as described in (C). Mean values ± SD; paired t test; n = 3 independent experiments.

(J) Percentage of SOX6 or OTX2 expressing TH^+ neurons differentiated in the presence of IWP2 and treated with either DMSO or rotenone (100 nM) for 48 h at day 35. Mean values ± SD; paired t test; n = 3 independent experiments.

(K) Relative levels of *TH* expression in toxin-treated neurons compared with untreated (normalized to 1). Mean values ± SD; one-way ANOVA with Bonferroni correction; n = 3 independent experiments.

*p < 0.05, **p < 0.01, ***p < 0.001. Scale bars, 200 μm (A), 100 μm (E), and 50 μm (C, F, and I).

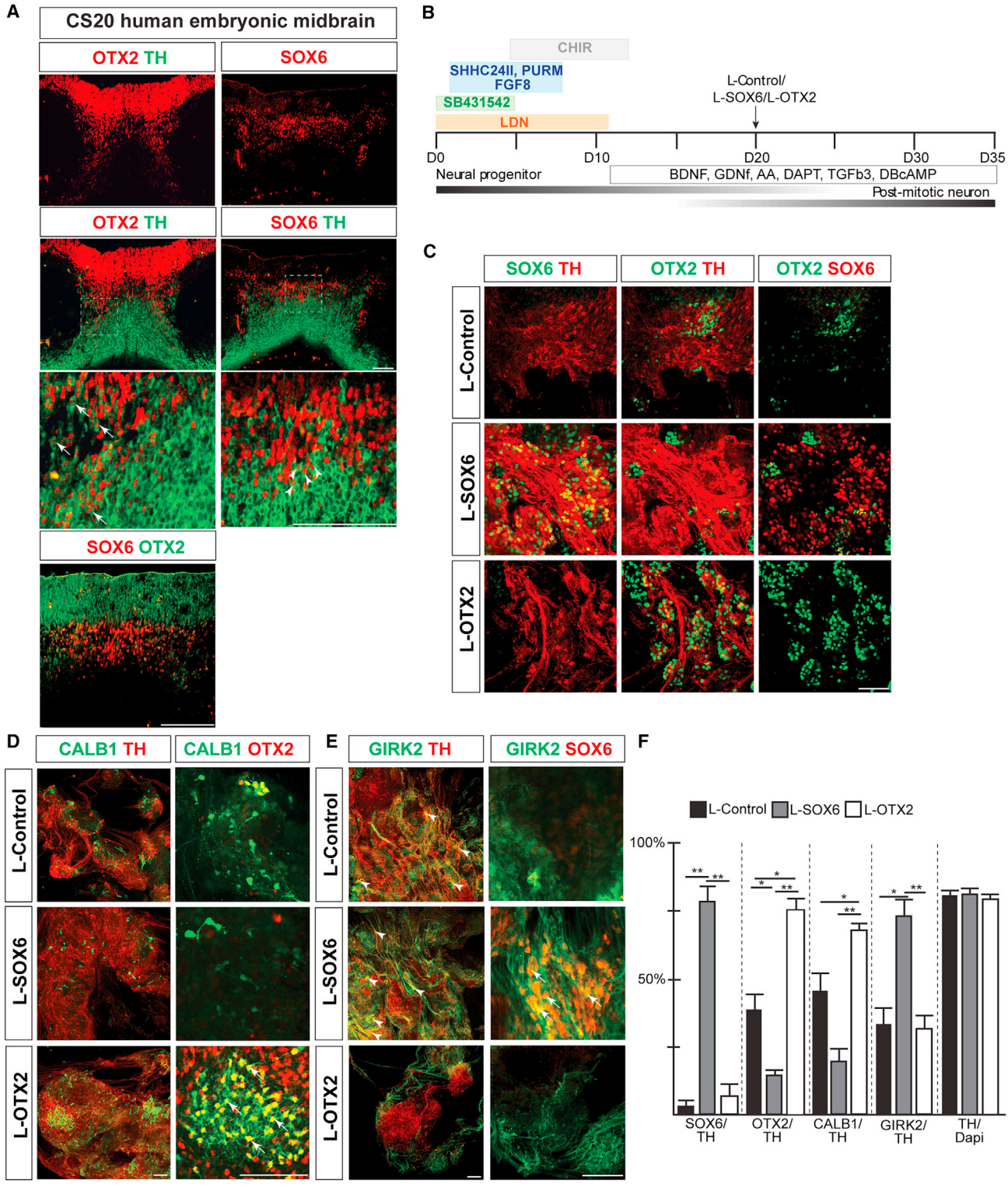

Figure 5. Induction of DA-subpopulation-specific markers in dopaminergic cultures transduced with L-SOX6 and L-OTX2

(A) IHC analysis of coronal sections of the human embryonic midbrain. Arrows indicate OTX2$^+$ DA neurons, while arrowheads point to SOX6$^+$ DA neurons. Higher-magnification images are from the regions indicated by a dashed square.

(B) Schematic overview of differentiation conditions. Arrow indicates time point of lentiviral transduction.

(legend continued on next page)

(15% versus 40% in controls) (Figures 5C and 5F) and CALB1 (21% versus 41% in controls) (Figures 5D and 5F). In contrast, transduction with OTX2 resulted in an increased number of TH^+ neurons expressing the VTA-specific marker CALB1 (67%) (Figures 5D and 5F) and a reduction of GIRK2 expression (32%) (Figures 5E and 5F). Midbrain identity (Figures S6B and S6C) and TH^+ cell numbers (Figure 5F) remained unaffected by lentiviral overexpression. These results demonstrate that we can direct the differentiation of hESCs toward enriched cultures for mDA neurons that display either SN- or VTA-like subtype identities using lineage-specific transcription factors. In addition, similar outcomes were obtained when using the AST iPSC line (Devine et al., 2011), showing an increased expression of SOX6 and GIRK2 upon L-SOX6 transduction (Figures S5E and S5I) and a reciprocal increase of VTA-specific markers OTX2 and CALB1 with L-OTX2 (Figures S5E, S5G, and S5I). Interestingly, there was a dramatic increase in α-SYNUCLEIN (α-SYN) expression in neurons transduced with SOX6 (Figures S5F and S5H), indicating that our strategy can be used to reveal genotypic and cell-type-specific disease phenotypes in iPSCs.

Sox6 induction confers vulnerability to human PSC-derived dopaminergic neurons

To provide a further link between SOX6 induction, acquisition of SN-like identities, and selective vulnerability, we examined the effect of mitochondrial toxins on lentiviral transduced cultures. hESC-derived dopaminergic neurons transduced with either L-Control, L-SOX6, or L-OTX2 (Figure 5B) were treated with rotenone for 24 h at day 35 and assayed for cell viability. In contrast to control and L-OTX2 transduced cultures, we observed elevated levels of cCASP3 and a reduction in numbers of TH^+ neurons in L-SOX6 transduced cultures after exposure to rotenone (Figures 6A and 6C). The difference in sensitivity between virus transduced cultures was further confirmed by the selective loss of viable cells in L-SOX6 transduced neurons, as indicated by a reduction in cellular ATP content (Figures 6D and S5J). Although higher concentrations of rotenone (100 nM) also caused a reduction of *TH* expression in control cultures as revealed by qPCR analysis, the reduction was more striking in L-SOX6 transduced neurons and not observed in L-OTX2 transduced cultures, consistent with the suggested role for OTX2 in neuroprotection (Di Salvio et al., 2010) (Figure 6E). Remarkably, in L-SOX6 transduced cultures the number of SOX6-labeled DA neurons was drastically reduced upon rotenone treatment (Figures 6B and 6F), while OTX2 expression was maintained in L-OTX2 transduced cultures. The formation of an excess amount of reactive oxygen species (ROS) contributes to the selective degeneration of SN neurons (Dias et al., 2013). Rotenone caused a strong increase in ROS production selectively in L-SOX6 transduced cultures (Figures S6D and S6E). Similar results were obtained with the mitochondrial inhibitor MPP^+, which is more efficiently taken up by SN neurons (Di Salvio et al., 2010). Forced expression of SOX6 in DA neurons resulted in increased sensitivity to MPP^+ (20 μM for 96 h) with elevated levels of cCASP3 and a reduction in TH expression (Figures S6F, S6H, and S6I). cCASP3 was upregulated in the nuclei of SOX6-expressing neurons after MPP^+ treatment, consistent with the increased susceptibility of these neurons to undergo apoptosis (Figure S6F). Consistent with the higher resistance of VTA neurons to mitochondrial toxicity, exposure to 20 μM MPP^+ for 96 h did not have any effect on control and L-OTX2 transduced cultures (Figures S6G–S6I).

Proteins involved in metabolism are enriched in Sox6-induced SN-like neurons

To understand how SOX6 renders DA more vulnerable, we determined the protein species induced by SOX6. Therefore, DA neuronal cultures were transduced with L-Control, L-SOX6, and L-OTX2 (Figure 5B), and differences in protein expression between the cultures were determined at day 35 (Table S2) by mass spectrometry using label-free quantitative methods. We identified several proteins that are differently expressed between L-SOX6 and L-OTX2 transduced cultures (Figure 7A; fold change [FC] > 2; $p < 0.05$). Western blot analysis confirmed these results and showed the expected induction of SOX6 and OTX2 in L-SOX6 and L-OTX2 transduced samples, respectively (Figures S7A and S7B). Pathway analysis showed an enrichment of proteins involved in metabolism and glycolysis in L-SOX6 transduced neurons (Figure 7B), consistent with the reported higher rate of glycolysis in SN neurons needed for ATP production (Pacelli et al., 2015). The expression of the proteins involved in metabolism was further validated by *in situ* hybridization and immunohistochemistry and confirmed that VAT1, GOT1, PGAM1, glucose-6-phosphate isomerase (GPI), and ALDOC are more highly expressed in the SN of the 18-week-old human fetal or embryonic day 18.5

(C) IHC analysis of day-35 lentiviral transduced cultures.
(D) IHC analysis of lentivirus transduced cultures (day 35). Arrowheads indicate overlap between CALB1 and OTX2.
(E) IHC analysis of lentivirus transduced cultures at day 35. Arrowheads indicate overlap between GIRK2 and SOX6.
(F) Graph showing percentage of TH^+ neurons expressing indicated markers at day 35. Mean ± SD; one-way ANOVA with Bonferroni correction; n = 3 independent experiments.
*$p < 0.05$, **$p < 0.01$. Scale bars, 100 μm.

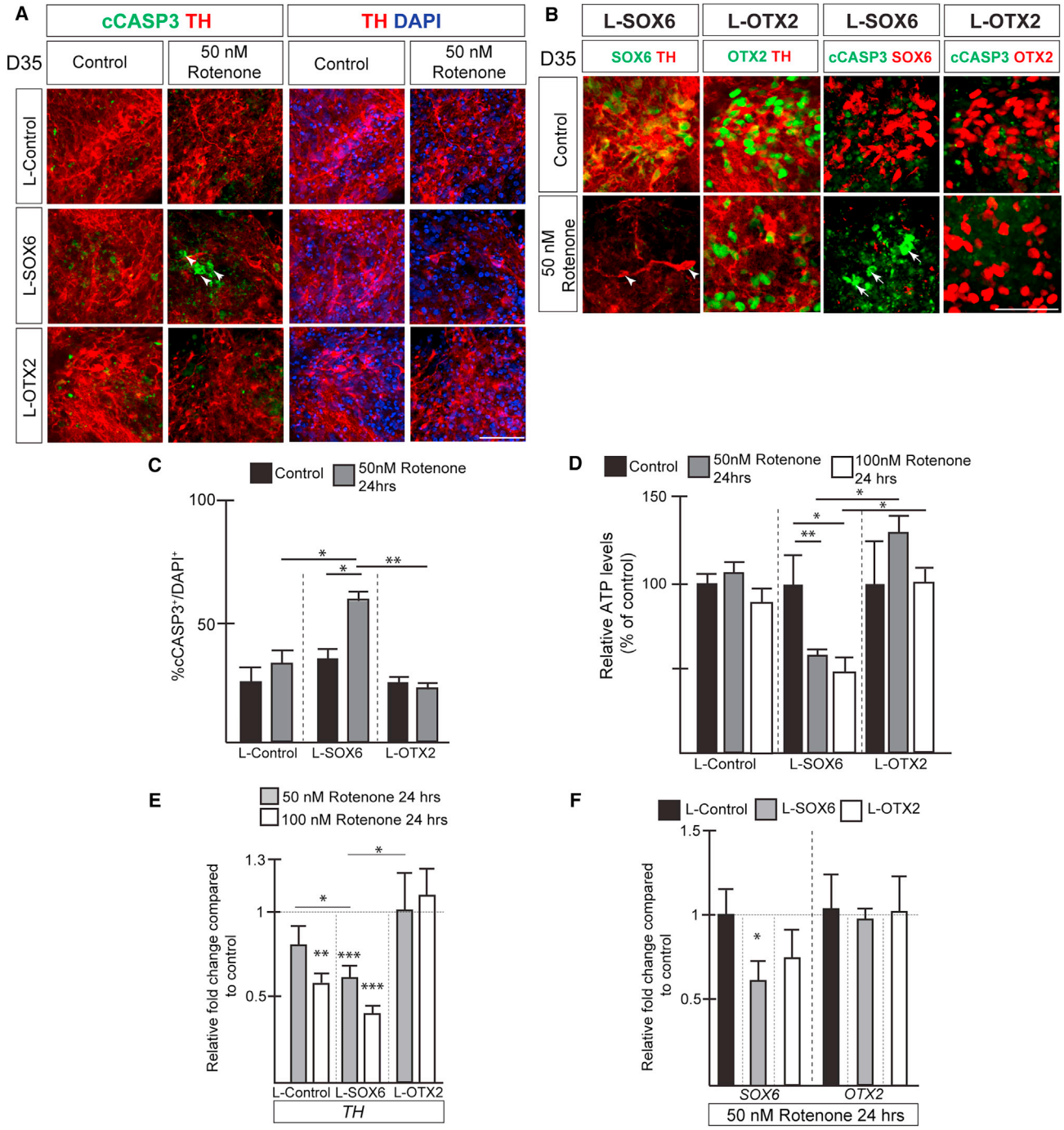

Figure 6. L-Sox6 transduced dopaminergic neurons display increased sensitivity to rotenone

(A) IHC analysis of lentiviral transduced cultures treated with rotenone at day 35 for 24 h. Arrowheads indicate cCASP3-expressing cells.

(B) Immunohistochemical analysis shows loss of SOX6 expression (arrowheads) and increase in cCASP3 (arrows) expression in L-SOX6 transduced cultures upon rotenone treatment.

(C) Graph displaying % percentage of $CASP3^{+}/DAPI^{+}$ in virus transduced control and 50 nM rotenone (24 h)-treated cultures at day 35. Mean ± SD; one-way ANOVA with Bonferroni correction; n = 3.

(D) Relative ATP levels in rotenone-treated cultures (24 h, day 35) as a percentage of the untreated cultures. Mean ± SD; one-way ANOVA with Bonferroni correction; n = 4 independent experiments.

(legend continued on next page)

(E18.5) mouse midbrain (Figures S7C and S7D). To gain insight into the requirement of glycolysis in SN-like DA neuron-enriched cultures, we decided to pharmacologically interfere with the levels of glycolysis. We used 6-phosphogluconic acid (6PG), an inhibitor of GPI (Parr, 1956) and meclizine (Gohil et al., 2010), to reduce and elevate, respectively, the rate of glycolysis in hESC- and mESC-derived SN-like DA neuronal cultures. While addition of 10 μM 6PG for 24 h at day 35 had only a very minor effect on cell viability in L-SOX6 hESC-derived DA cultures (Figure 7D), its combination with 50 nM rotenone synergistically reduced the cellular ATP levels (Figure 7D), induced cCASP3 expression, and decreased the number of TH- and SOX6-positive neurons (Figure 7C). In contrast, L-Control and L-OTX2 transduced cultures were relatively unaffected after reducing both glycolysis and oxidative phosphorylation (Figure 7D). Next, we examined whether enhancement of glycolysis using meclizine protects L-SOX6 transduced cultures against mitochondrial toxicity. Remarkably, the effects of rotenone on cell survival were reversed by the addition of meclizine at the same time, decreasing the levels of cCASP3 and increasing SOX6 expression (Figures 7C and 7E). Similar effects of meclizine were obtained in mouse mFP-derived DA cultures. Rotenone treatment of SOX6-enriched DA cultures resulted in increased levels of cCASP3 (Figure 7F) and a reduction of TH^+ cells (Figure 7G). However, treatment with meclizine reversed the effects of rotenone on neuronal cell death, and levels of TH expression were significantly increased (Figures 7F and 7G). This comparative protein expression analysis has revealed several targetable proteins and pathways that could be used for future studies to discover novel strategies to prevent neurodegeneration.

DISCUSSION

Neurodegenerative diseases typically affect a selective population of neurons (Roselli and Caroni, 2015), and the ability to generate these disease-relevant neuronal subtypes *in vitro* will offer important opportunities for disease modeling and drug discovery. Here we showed that the differentiation of mouse and human PSC-derived DA progenitors can be directed toward the SN-like neuronal lineage either through WNT inhibitor-mediated induction of mFP cells or by forced expression of SOX6 (Figure 7H). The obtained cultures displayed the selective sensitivity of SN neurons to mitochondrial toxins, while cultures mainly consisting of DA neurons with VTA-like identities were more resistant (Figure 7H). Our approach demonstrates that the differential vulnerability of DA neurons can be reproduced in PSC-derived cultures, providing a platform for modeling PD.

Published mouse and human PSC differentiation protocols give rise to a mixture of DA neurons with SN- and VTA-specific neuronal identities (Friling et al., 2009; Grealish et al., 2014; Kriks et al., 2011). Here we described how cultures enriched for a specific subpopulation can be obtained *in vitro*. We found that SN- and VTA-like neuronal lineages are derived from distinct DA progenitor populations during PSC differentiation, as observed during embryonic development (Blaess et al., 2011; Panman et al., 2014). mESC differentiation conditions that promoted the specification of medial progenitor (mFP) cells resulted in the efficient induction of the SN lineage-associated marker Sox6 in nearly all DA neurons. In contrast, lateral DA progenitors were generated under culture conditions that promote the specification of DA neurons with mainly VTA-like identities (Figure 7H). Consistent with mouse studies (Nouri et al., 2015; Yang et al., 2013), our data suggest that specification of these distinct lateral and medial progenitor populations is mediated by differential WNT/β-CATENIN signaling during DA progenitor differentiation. First, mESCs differentiated according to the mFP protocol, which give rise to the SN-like neuronal lineage, showed lower levels of endogenous canonical WNT signaling at the progenitor stage. Second, WNT signaling inhibition resulted in a lateral to medial switch of DA progenitor identity, which promoted the acquisition of SN-like specific identities in DA cultures. Third, activation of WNT signaling directed the differentiation toward the VTA-like neuronal lineage.

The timing and concentration of growth factor addition to PSC-derived cultures are important determinants of the differentiation outcome, as shown for several neuronal populations including cortical, motor, and serotonergic neurons (Tao and Zhang, 2016). The pleiotropic role of WNT signaling in mDA neuron development underlines the importance for defining optimal concentrations and time points for adding WNT signaling inhibitors. We defined that the critical window for IWP2-mediated induction of SOX6 in human PSC-derived DA neurons is from day 11 to day 16, once DA progenitors have been fully specified (Kriks et al., 2011). The addition of WNT inhibitors before DA progenitors have been fully specified will

(E) qPCR analysis of *TH* expression in rotenone-treated (24 h, day 35) virus transduced cultures compared with untreated cultures (normalized to 1). Mean ± SD; one-way ANOVA with Bonferroni correction; n = 4 independent experiments.
(F) qPCR analysis of *SOX6* and *OTX2* expression in rotenone-treated (24 h, day 35) virus transduced cultures compared with untreated cultures (normalized to 1). Mean ± SD; unpaired t test; n = 4 independent experiments.
*p < 0.05, **p < 0.01. Scale bars, 50 μm.

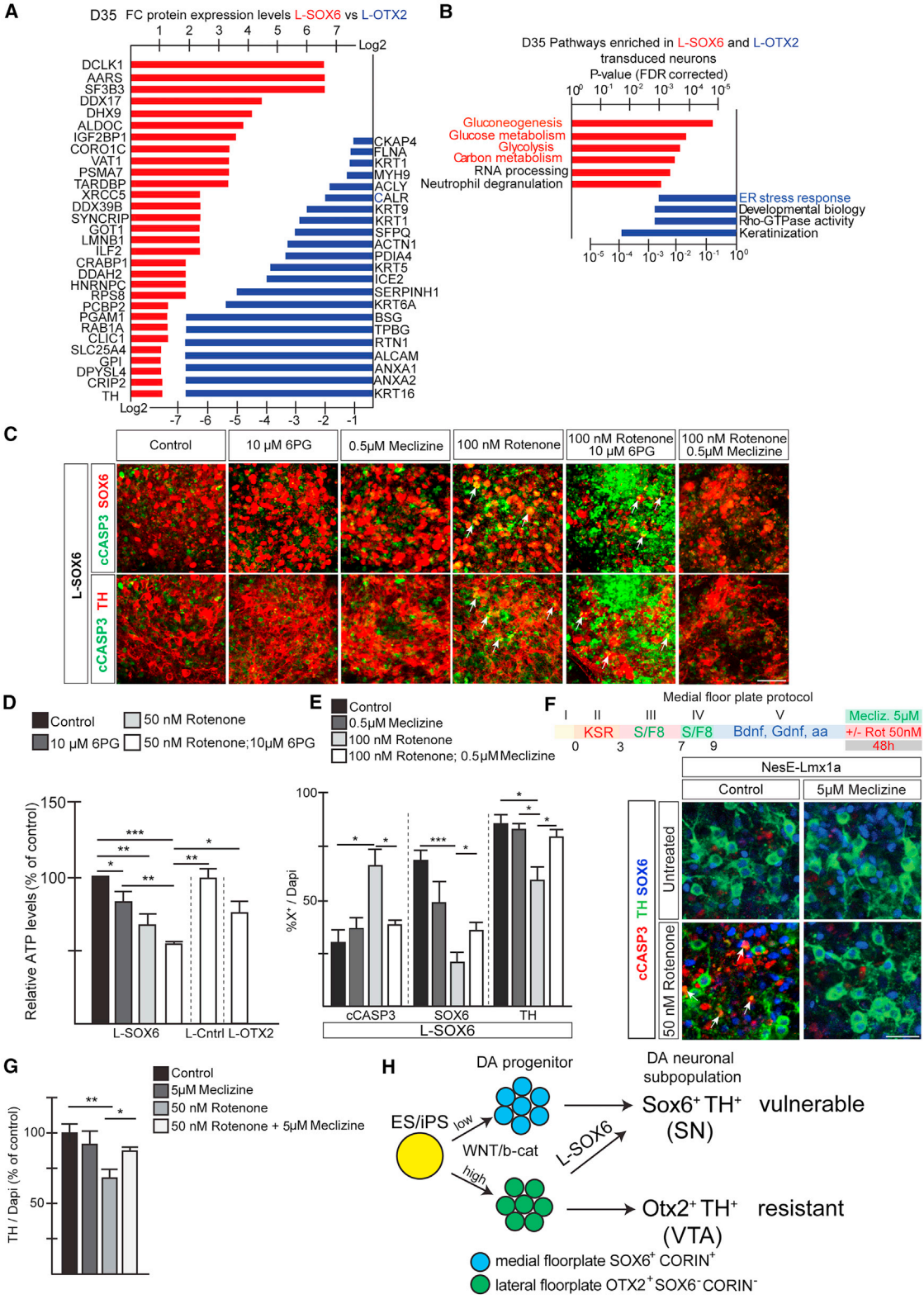

(legend on next page)

interfere with DA neuron production (Kee et al., 2017; Kirkeby et al., 2012; Kriks et al., 2011; Nolbrant et al., 2017). Extending the exposure time to IWP2 strongly reduces DA cell numbers, which is consistent with the later requirement of canonical WNT signaling for DA neuron survival (L'Episcopo et al., 2011; Zhang et al., 2015).

Although we were able to guide the mESC differentiation toward the SN-like neuronal lineage using extrinsic factors in the mFP protocol, the addition of Wnt signaling inhibitors alone did not result in a complete lineage conversion in human ESC-derived DA progenitors. Other signaling pathways, including bone morphogenetic protein, transforming growth factor α, and SHH (Blaess et al., 2011; Blum, 1998; Jovanovic et al., 2018), may cooperate with WNT in specifying subpopulation identity. Transcription factor overexpression has been successfully applied previously to overcome these hurdles and efficiently generates homogeneous neuronal populations even under non-permissive culture conditions (Au et al., 2013; Friling et al., 2009; Mazzoni et al., 2013; Mong et al., 2014; Panman et al., 2011). Indeed, forced expression of the lineage-specific transcription factor SOX6 in early human PSC-derived post-mitotic DA neurons resulted in an even more efficient induction of SN neuronal lineage markers than obtained after addition of WNT inhibitors.

In this study, the achieved enrichment for SN neuronal lineage markers conferred sensitivity to mitochondrial toxins in both mouse and human PSC-derived DA cultures, which was not observed under standard differentiation conditions. Our results demonstrate that the culture-dependent sensitivity is directly related to the molecular identity of the obtained neurons, providing a functional verification of PSC-derived DA subpopulations. Indeed, exposure to MPP^+ and rotenone resulted in apoptosis, reduction in ATP levels, and increased ROS production selectively in SN-like enriched cultures, consistent with *in vivo* models of PD. Interestingly, in particular SOX6-expressing neurons were affected upon toxin exposure with cCASP3 overlapping with SOX6 in the nucleus. This effect was reversed when levels of SOX6 were downregulated either by CHIR treatment or high-dose SHH conditions. Thus, the induced sensitivity correlated with the presence of SOX6-labeled DA neurons and was not caused by modified culture conditions. Since SN and VTA DA neurons have specialized functions and are associated with distinct neurological disorders, our platform will be highly amenable for PD disease modeling *in vitro*.

Comparative protein analysis between L-SOX6 and L-OTX2 transduced cultures revealed several subpopulation-specific features that could underlie the differences in vulnerability. Consistent with the higher metabolic demand of SN neurons (Bolam and Pissadaki, 2012; Pacelli et al., 2015), pathway analysis revealed an enrichment for proteins involved in glycolysis and glucose metabolism. Indeed, it has been shown previously that the glycolytic rate is higher in SN neurons compared with the VTA and is further increased after blocking mitochondrial respiration to compensate for the loss of ATP production (Chaudhuri et al., 2015; Pacelli et al., 2015). We demonstrated that blocking glycolysis with the GPI antagonist 6PG exacerbated the effects of rotenone selectively in L-SOX6 transduced cultures. Furthermore, enhancing glycolysis with meclizine (Gohil et al., 2010) prevents the induction of cCASP3 and increases cell viability in SN-like neurons after mitochondrial toxic insult. Although the molecular targets are currently unknown, meclizine is a Food and Drug Administration-approved drug crossing the blood-brain barrier and therefore may hold therapeutic potential in the treatment of PD and other neurodegenerative diseases.

Finally, our *in vitro* platform provides a unique approach for modeling selective neuronal vulnerability in PD and could be applied to other neurodegenerative diseases, including amyotrophic lateral sclerosis and Alzheimer's disease. It lays a framework for examining mechanisms underlying selective neuronal cell death in general and will facilitate the discovery of genes and drugs that modulate

Figure 7. SOX6-mediated induction of metabolic pathways provides protection of neurons to mitochondrial toxicity

(A) Proteins differentially expressed between L-SOX6 (red bars) and L-OTX2 (blue bars) transduced hESC-derived cultures (day 35). Expression levels are presented as $\log_2$ transformed fold change (FC) values.

(B) Graph indicates pathways significantly enriched in L-SOX6 and L-OTX2 transduced cultures.

(C) IHC analysis of L-SOX6 transduced hESC-derived cultures treated as indicated for 24 h at day 35. Arrows indicate cCASP3-labeled SOX6- and TH-expressing neurons.

(D) Relative ATP levels in rotenone- and 6PG-treated cultures (24 h, day 35) as a percentage of the untreated cultures. Mean ± SD; one-way ANOVA with Bonferroni correction; n = 4 independent experiments.

(E) Percentage of cCASP3-, SOX6-, and TH-expressing cells in hESC-derived L-SOX6 transduced cultures treated with rotenone and meclizine (24 h, day 35). Mean ± SD; one-way ANOVA with Bonferroni correction; n = 4 independent experiments.

(F) mESC differentiation scheme. IHC analysis of Nes-Lmx1a mESC-derived cultures. Arrows indicate overlap between cCASP3 and TH.

(G) Percentage of TH^+ neurons present in mESC medial FP-derived cultures. Control value normalized to 100. Mean ± SD; one-way ANOVA with Bonferroni correction; n = 4 independent experiments.

(H) Model illustrating DA sublineage selection process during mouse and human PSC differentiation and its consequences on vulnerability.

*p < 0.05, **p < 0.01, ***p < 0.001. Scale bars, 50 μm.

these differences in sensitivity to disease. The established differentiation protocols can be used to further explore the mechanisms controlling DA diversity during ESC differentiation using SOX6 and OTX2 in combination with other early subpopulation-specific markers.

EXPERIMENTAL PROCEDURES

Detailed descriptions of the experimental procedures can be found in the supplemental information.

Maintenance and differentiation of mouse ESCs

Wild-type E14.1 and NesE-Lmx1a mouse ESC lines were propagated on MEF cells as previously described (Friling et al., 2009; Panman et al., 2011) in the presence of LIF. Mouse ESCs were differentiated according to the 5-stage protocol as previously described (Lee et al., 2000) with some minor modifications. For the mFP protocol, basic FGF, FGF8, and SAG1.3 were added to stage III.

Maintenance and differentiation of hESCs and iPSCs

Human ESCs H9 (WA09, passage 32–48) (Thomson et al., 1998) and iPSCs AST23 (Edi001-A ECACC cat. no. 66540058, passage 25–35) (Devine et al., 2011) were cultured on Geltrex-coated 6-well plates in Essential 8 medium (Gibco) as described by the manufacturer's protocol. hESCs and iPSCs were differentiated according to the FP protocol (Kriks et al., 2011) with some minor modifications.

Quantitative mass spectrometry analysis

For each condition, three independent biological replicates were obtained. Each sample was divided over three lanes and migrated on a 10% SDS-PAGE gel. The gel was stained with Coomassie blue and each lane was subsequently cut horizontally in three bands and in-gel digested with bovine trypsin (Roche). All experiments were performed on a dual linear ion trap Fourier transform mass spectrometer.

Data and code availability

The mass spectrometry proteomics data have been deposited in the ProteomeXchange Consortium (http://www.proteomexchange.org) via the PRIDE partner repository with the dataset identifier PXD028639.

SUPPLEMENTAL INFORMATION

Supplemental information can be found online at https://doi.org/10.1016/j.stemcr.2021.09.014.

AUTHOR CONTRIBUTIONS

T.O. and L.P. conceived and designed the research project; T.O., P.G., E.M.-G., C.S., M.T., R.P., K.P., V.L., L.C.-S., U.M., and L.P. performed experiments and collected and analyzed the data; S.S. and P.H. contributed new reagents; L.P. wrote the paper. All authors provided critical comments on the manuscript and results.

CONFLICTS OF INTEREST

The authors declare no competing interests.

ACKNOWLEDGMENTS

The human embryonic and fetal material were provided by the joint MRC/Wellcome Trust (grant #099175/Z/12/Z) Human Developmental Biology Resource (www.hdbr.org) and by Erik Sundström and the staff at the gynecology clinic, Karolinska University Hospital, Huddinge. We thank Daniel Hagey and Jonas Muhr for providing the SOX6 antibody. We thank A. Willis and lab members for discussions and providing comments on the manuscript. This work was supported by funding from the Medical Research Council (L.P., S.S.), ITTP (L.P.), Vetenskapsrådet (L.P., U.M.), Svenska Läkaresällskapet (U.M.), Parkinson's funden (L.P.), European Regional Development Fund (SMHART project 35069) (L.C., V.L.), Conseil Régional du Centre (L.C., V.L.), INRA (L.C., V.L.). and Inserm (L.C., V.L.), and the Biotechnology and Biological Sciences Research Council (P.H.). We thank Lucia Pinon and Paul Alexander for technical assistance.

Received: December 1, 2020
Revised: September 20, 2021
Accepted: September 21, 2021
Published: October 21, 2021

REFERENCES

Anderegg, A., Poulin, J.F., and Awatramani, R. (2015). Molecular heterogeneity of midbrain dopaminergic neurons—moving toward single cell resolution. FEBS Lett. *589*, 3714–3726.

Au, E., Ahmed, T., Karayannis, T., Biswas, S., Gan, L., and Fishell, G. (2013). A modular gain-of-function approach to generate cortical interneuron subtypes from ES cells. Neuron *80*, 1145–1158.

Blaess, S., Bodea, G.O., Kabanova, A., Chanet, S., Mugniery, E., Derouiche, A., Stephen, D., and Joyner, A.L. (2011). Temporal-spatial changes in Sonic Hedgehog expression and signaling reveal different potentials of ventral mesencephalic progenitors to populate distinct ventral midbrain nuclei. Neural Dev. *6*, 29.

Blum, M. (1998). A null mutation in TGF-alpha leads to a reduction in midbrain dopaminergic neurons in the substantia nigra. Nat. Neurosci. *1*, 374–377.

Bolam, J.P., and Pissadaki, E.K. (2012). Living on the edge with too many mouths to feed: why dopamine neurons die. Mov. Disord. *27*, 1478–1483.

Bove, J., Prou, D., Perier, C., and Przedborski, S. (2005). Toxin-induced models of Parkinson's disease. NeuroRx *2*, 484–494.

Chaudhuri, A.D., Kabaria, S., Choi, D.C., Mouradian, M.M., and Junn, E. (2015). MicroRNA-7 promotes glycolysis to protect against 1-methyl-4-phenylpyridinium-induced cell death. J. Biol. Chem. *290*, 12425–12434.

Chen, B., Dodge, M.E., Tang, W., Lu, J., Ma, Z., Fan, C.W., Wei, S., Hao, W., Kilgore, J., Williams, N.S., et al. (2009). Small molecule-mediated disruption of Wnt-dependent signaling in tissue regeneration and cancer. Nat. Chem. Biol. *5*, 100–107.

Chung, S., Leung, A., Han, B.S., Chang, M.Y., Moon, J.I., Kim, C.H., Hong, S., Pruszak, J., Isacson, O., and Kim, K.S. (2009). Wnt1-lmx1a forms a novel autoregulatory loop and controls midbrain dopaminergic differentiation synergistically with the SHH-FoxA2 pathway. Cell Stem Cell *5*, 646–658.

Devine, M.J., Ryten, M., Vodicka, P., Thomson, A.J., Burdon, T., Houlden, H., Cavaleri, F., Nagano, M., Drummond, N.J., Taanman, J.W., et al. (2011). Parkinson's disease induced pluripotent stem cells with triplication of the alpha-synuclein locus. Nat. Commun. *2*, 440.

Di Salvio, M., Di Giovannantonio, L.G., Acampora, D., Prosperi, R., Omodei, D., Prakash, N., Wurst, W., and Simeone, A. (2010). Otx2 controls neuron subtype identity in ventral tegmental area and antagonizes vulnerability to MPTP. Nat. Neurosci. *13*, 1481–1488.

Dias, V., Junn, E., and Mouradian, M.M. (2013). The role of oxidative stress in Parkinson's disease. J. Parkinsons Dis. *3*, 461–491.

Friling, S., Andersson, E., Thompson, L.H., Jonsson, M.E., Hebsgaard, J.B., Nanou, E., Alekseenko, Z., Marklund, U., Kjellander, S., Volakakis, N., et al. (2009). Efficient production of mesencephalic dopamine neurons by Lmx1a expression in embryonic stem cells. Proc. Natl. Acad. Sci. U S A *106*, 7613–7618.

Fu, Y., Yuan, Y., Halliday, G., Rusznak, Z., Watson, C., and Paxinos, G. (2012). A cytoarchitectonic and chemoarchitectonic analysis of the dopamine cell groups in the substantia nigra, ventral tegmental area, and retrorubral field in the mouse. Brain Struct. Funct. *217*, 591–612.

Gohil, V.M., Sheth, S.A., Nilsson, R., Wojtovich, A.P., Lee, J.H., Perocchi, F., Chen, W., Clish, C.B., Ayata, C., Brookes, P.S., et al. (2010). Nutrient-sensitized screening for drugs that shift energy metabolism from mitochondrial respiration to glycolysis. Nat. Biotechnol. *28*, 249–255.

Grealish, S., Diguet, E., Kirkeby, A., Mattsson, B., Heuer, A., Bramoulle, Y., Van Camp, N., Perrier, A.L., Hantraye, P., Bjorklund, A., et al. (2014). Human ESC-derived dopamine neurons show similar preclinical efficacy and potency to fetal neurons when grafted in a rat model of Parkinson's disease. Cell Stem Cell *15*, 653–665.

Jho, E.H., Zhang, T., Domon, C., Joo, C.K., Freund, J.N., and Costantini, F. (2002). Wnt/beta-catenin/Tcf signaling induces the transcription of Axin2, a negative regulator of the signaling pathway. Mol. Cell Biol. *22*, 1172–1183.

Jovanovic, V.M., Salti, A., Tilleman, H., Zega, K., Jukic, M.M., Zou, H., Friedel, R.H., Prakash, N., Blaess, S., Edenhofer, F., et al. (2018). BMP/SMAD pathway promotes neurogenesis of midbrain dopaminergic neurons in vivo and in human induced pluripotent and neural stem cells. J. Neurosci. *38*, 1662–1676.

Kee, N., Volakakis, N., Kirkeby, A., Dahl, L., Storvall, H., Nolbrant, S., Lahti, L., Bjorklund, A.K., Gillberg, L., Joodmardi, E., et al. (2017). Single-cell analysis reveals a close relationship between differentiating dopamine and subthalamic nucleus neuronal lineages. Cell Stem Cell *20*, 29–40.

Kirkeby, A., Grealish, S., Wolf, D.A., Nelander, J., Wood, J., Lundblad, M., Lindvall, O., and Parmar, M. (2012). Generation of regionally specified neural progenitors and functional neurons from human embryonic stem cells under defined conditions. Cell Rep. *1*, 703–714.

Kriks, S., Shim, J.W., Piao, J., Ganat, Y.M., Wakeman, D.R., Xie, Z., Carrillo-Reid, L., Auyeung, G., Antonacci, C., Buch, A., et al. (2011). Dopamine neurons derived from human ES cells efficiently engraft in animal models of Parkinson's disease. Nature *480*, 547–551.

L'Episcopo, F., Serapide, M.F., Tirolo, C., Testa, N., Caniglia, S., Morale, M.C., Pluchino, S., and Marchetti, B. (2011). A Wnt1 regulated Frizzled-1/beta-Catenin signaling pathway as a candidate regulatory circuit controlling mesencephalic dopaminergic neuron-astrocyte crosstalk: therapeutical relevance for neuron survival and neuroprotection. Mol. Neurodegener. *6*, 49.

Lee, S.H., Lumelsky, N., Studer, L., Auerbach, J.M., and McKay, R.D. (2000). Efficient generation of midbrain and hindbrain neurons from mouse embryonic stem cells. Nat. Biotechnol. *18*, 675–679.

Marklund, U., Alekseenko, Z., Andersson, E., Falci, S., Westgren, M., Perlmann, T., Graham, A., Sundstrom, E., and Ericson, J. (2014). Detailed expression analysis of regulatory genes in the early developing human neural tube. Stem Cells Dev. *23*, 5–15.

Mazzoni, E.O., Mahony, S., Closser, M., Morrison, C.A., Nedelec, S., Williams, D.J., An, D., Gifford, D.K., and Wichterle, H. (2013). Synergistic binding of transcription factors to cell-specific enhancers programs motor neuron identity. Nat. Neurosci. *16*, 1219–1227.

Mong, J., Panman, L., Alekseenko, Z., Kee, N., Stanton, L.W., Ericson, J., and Perlmann, T. (2014). Transcription factor-induced lineage programming of noradrenaline and motor neurons from embryonic stem cells. Stem Cells *32*, 609–622.

Nakamura, R.E., and Hackam, A.S. (2010). Analysis of Dickkopf3 interactions with Wnt signaling receptors. Growth Factors *28*, 232–242.

Nolbrant, S., Heuer, A., Parmar, M., and Kirkeby, A. (2017). Generation of high-purity human ventral midbrain dopaminergic progenitors for in vitro maturation and intracerebral transplantation. Nat. Protoc. *12*, 1962–1979.

Nouri, N., Patel, M.J., Joksimovic, M., Poulin, J.F., Anderegg, A., Taketo, M.M., Ma, Y.C., and Awatramani, R. (2015). Excessive Wnt/beta-catenin signaling promotes midbrain floor plate neurogenesis, but results in vacillating dopamine progenitors. Mol. Cell Neurosci. *68*, 131–142.

Pacelli, C., Giguere, N., Bourque, M.J., Levesque, M., Slack, R.S., and Trudeau, L.E. (2015). Elevated mitochondrial bioenergetics and axonal arborization size are key contributors to the vulnerability of dopamine neurons. Curr. Biol. *25*, 2349–2360.

Panman, L., Andersson, E., Alekseenko, Z., Hedlund, E., Kee, N., Mong, J., Uhde, C.W., Deng, Q., Sandberg, R., Stanton, L.W., et al. (2011). Transcription factor-induced lineage selection of stem-cell-derived neural progenitor cells. Cell Stem Cell *8*, 663–675.

Panman, L., Papathanou, M., Laguna, A., Oosterveen, T., Volakakis, N., Acampora, D., Kurtsdotter, I., Yoshitake, T., Kehr, J., Joodmardi, E., et al. (2014). Sox6 and Otx2 control the specification of substantia nigra and ventral tegmental area dopamine neurons. Cell Rep. *8*, 1018–1025.

Parr, C.W. (1956). Inhibition of phosphoglucose isomerase. Nature *178*, 1401.

Poulin, J.F., Zou, J., Drouin-Ouellet, J., Kim, K.Y., Cicchetti, F., and Awatramani, R.B. (2014). Defining midbrain dopaminergic neuron diversity by single-cell gene expression profiling. Cell Rep. *9*, 930–943.

Poulin, J.F., Gaertner, Z., Moreno-Ramos, O.A., and Awatramani, R. (2020). Classification of midbrain dopamine neurons using single-cell gene expression profiling approaches. Trends Neurosci. *43*, 155–169.

Prakash, N., Brodski, C., Naserke, T., Puelles, E., Gogoi, R., Hall, A., Panhuysen, M., Echevarria, D., Sussel, L., Weisenhorn, D.M., et al. (2006). A Wnt1-regulated genetic network controls the identity and fate of midbrain-dopaminergic progenitors in vivo. Development *133*, 89–98.

Reyes, S., Fu, Y., Double, K., Thompson, L., Kirik, D., Paxinos, G., and Halliday, G.M. (2012). GIRK2 expression in dopamine neurons of the substantia nigra and ventral tegmental area. J. Comp. Neurol. *520*, 2591–2607.

Ribeiro, D., Ellwanger, K., Glagow, D., Theofilopoulos, S., Corsini, N.S., Martin-Villalba, A., Niehrs, C., and Arenas, E. (2011). Dkk1 regulates ventral midbrain dopaminergic differentiation and morphogenesis. PLoS One *6*, e15786.

Roselli, F., and Caroni, P. (2015). From intrinsic firing properties to selective neuronal vulnerability in neurodegenerative diseases. Neuron *85*, 901–910.

Smidt, M.P., and Burbach, J.P. (2007). How to make a mesodiencephalic dopaminergic neuron. Nat. Rev. Neurosci. *8*, 21–32.

Surmeier, D.J., Obeso, J.A., and Halliday, G.M. (2017). Selective neuronal vulnerability in Parkinson disease. Nat. Rev. Neurosci. *18*, 101–113.

Tao, Y., and Zhang, S.C. (2016). Neural subtype specification from human pluripotent stem cells. Cell Stem Cell *19*, 573–586.

Thomson, J.A., Itskovitz-Eldor, J., Shapiro, S.S., Waknitz, M.A., Swiergiel, J.J., Marshall, V.S., and Jones, J.M. (1998). Embryonic stem cell lines derived from human blastocysts. Science *282*, 1145–1147.

Tiklova, K., Bjorklund, A.K., Lahti, L., Fiorenzano, A., Nolbrant, S., Gillberg, L., Volakakis, N., Yokota, C., Hilscher, M.M., Hauling, T., et al. (2019). Single-cell RNA sequencing reveals midbrain dopamine neuron diversity emerging during mouse brain development. Nat. Commun. *10*, 581.

Yang, J., Brown, A., Ellisor, D., Paul, E., Hagan, N., and Zervas, M. (2013). Dynamic temporal requirement of Wnt1 in midbrain dopamine neuron development. Development *140*, 1342–1352.

Ying, Q.L., Stavridis, M., Griffiths, D., Li, M., and Smith, A. (2003). Conversion of embryonic stem cells into neuroectodermal precursors in adherent monoculture. Nat. Biotechnol. *21*, 183–186.

Ying, Q.L., Wray, J., Nichols, J., Batlle-Morera, L., Doble, B., Woodgett, J., Cohen, P., and Smith, A. (2008). The ground state of embryonic stem cell self-renewal. Nature *453*, 519–523.

Zhang, J., Gotz, S., Vogt Weisenhorn, D.M., Simeone, A., Wurst, W., and Prakash, N. (2015). A WNT1-regulated developmental gene cascade prevents dopaminergic neurodegeneration in adult En1(+/-) mice. Neurobiol. Dis. *82*, 32–45.

Stem Cell Reports, Volume *16*

Supplemental Information

Pluripotent stem cell derived dopaminergic subpopulations model the selective neuron degeneration in Parkinson's disease

Tony Oosterveen, Pedro Garção, Emma Moles-Garcia, Clement Soleilhavoup, Marco Travaglio, Shahida Sheraz, Rosa Peltrini, Kieran Patrick, Valerie Labas, Lucie Combes-Soia, Ulrika Marklund, Peter Hohenstein, and Lia Panman

Supplemental information

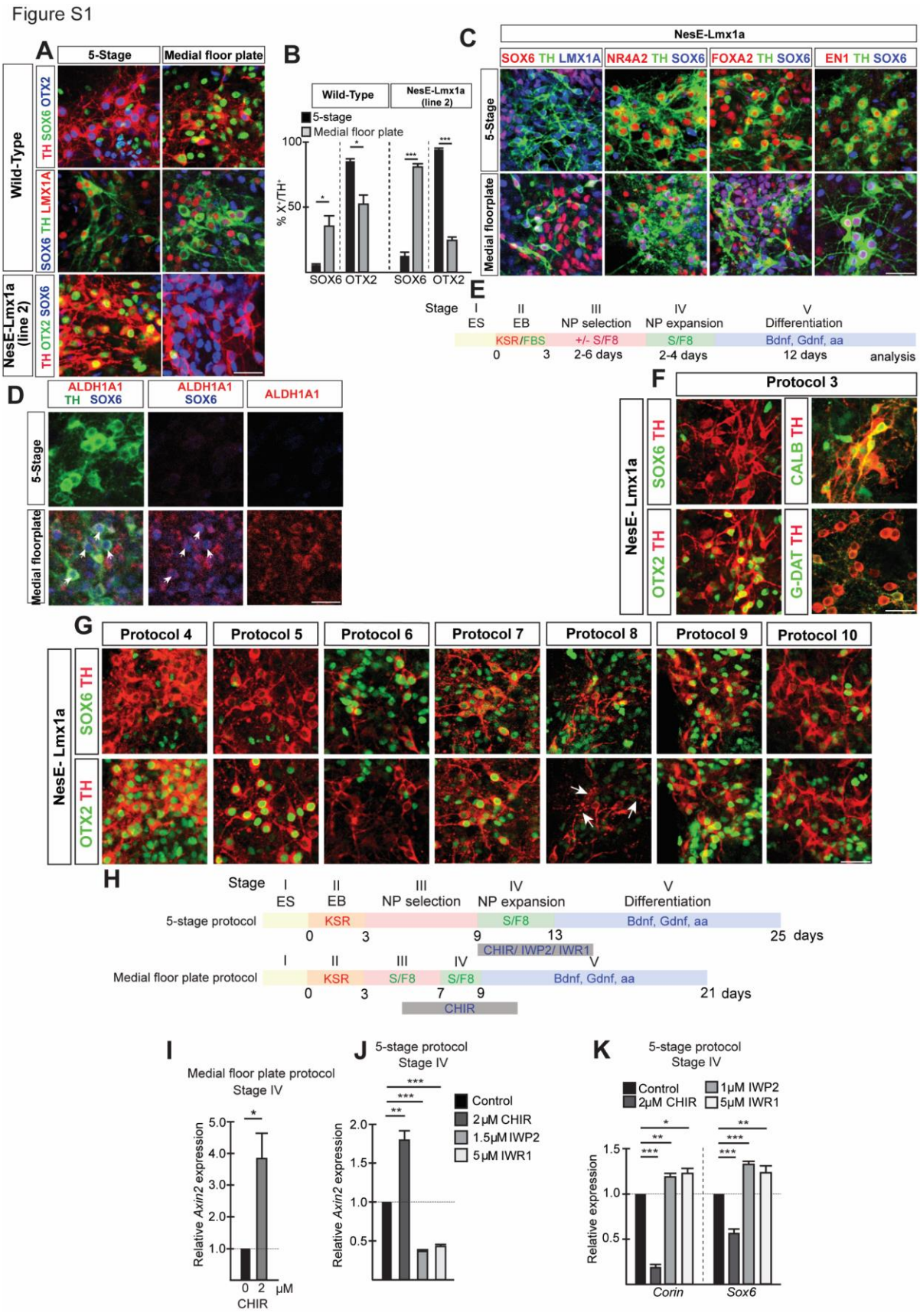

Figure S1 related to Figures 1 and 2. Different variants of the 5-stage protocol and the effect of Wnt signalling modulation on differentiation outcome. (A) Expression of DA markers in wild-type and NesE-Lmx1a (line 2) mES cell derived cultures differentiated according the 5-stage and medial floor plate protocols. (**B**) Percentage of SOX6 and OTX2 expressing TH positive neurons in wild-type mES cell and NesE-Lmx1a (line 2) derived cultures from indicated protocols (n = 3 independent experiments); mean values ± SD; unpaired ttest. **(C)** Marker analysis of NesE-Lmx1a ES cells derived TH labelled DA neurons obtained with the 5-stage and medial floor plate protocols. **(D)** Immunohistochemical analysis of ALDH1A1 in TH^+ neurons derived from NesE-Lmx1a mES cells obtained with the medial floor plate and 5-stage protocol. Arrows indicate $TH^+/SOX6^+$ neurons expressing ALDH1A1. **(E)** Diagram schematically presenting the different variations of the 5-stage protocol. **(F)** Immunohistochemical analysis of SOX6, OTX2, CALB1 and Glyco-DAT expression in TH^+ neurons derived from NesE-Lmx1a mES cells. FBS was used during EB formation in the 5-stage protocol (protocol 3). **(G)** Analysis of SOX6 and OTX2 expression in NesE-Lmx1a mES cell derived TH^+ neurons. mES cells were differentiated by different variants on the 5-stage protocol (see **E** and Table S1). Note reduced TH^+ cell numbers in cultures differentiated according to protocols 6 and 8. Arrows in protocol 8 indicate deficiently developed SOX6-positive neurons. **(H)** Diagrams showing the timing of CHIR, IWP2 and IWR1 addition in the 5-stage and medial floor-plate protocols. **(I)** Relative gene-expression levels of *Axin2* in NesE-Lmx1a mES cell derived DA progenitors differentiated according to the mFP protocol (Stage IV) upon 4 days exposure to CHIR (Stages III/IV) determined by qPCR (n=3 independent experiments). Mean values ± SD; unpaired ttest. **(J)** Relative gene-expression levels of *Axin2* in NesE-Lmx1a mES cell derived DA progenitors (Stage IV) differentiated according to the 5-stage protocol upon 4 days exposure to CHIR, IWP2 and IWR1 (Stage IV)

determined by qPCR (n=3 independent experiments). Mean values ± SD; one-way ANOVA with Bonferroni correction. **(K)** Relative gene-expression levels of *Corin* and *Sox6* in 5-stage protocol derived DA progenitor cells (Stage IV) exposed to Wnt signalling modulators for 4 days (Stage IV) determined by qPCR (n=3 independent experiments). Mean values ± SD; one-way ANOVA with Bonferroni correction. *$p < 0.05$, **$p < 0.01$, ***$p < 0.001$. Scale bar: 50 μM.

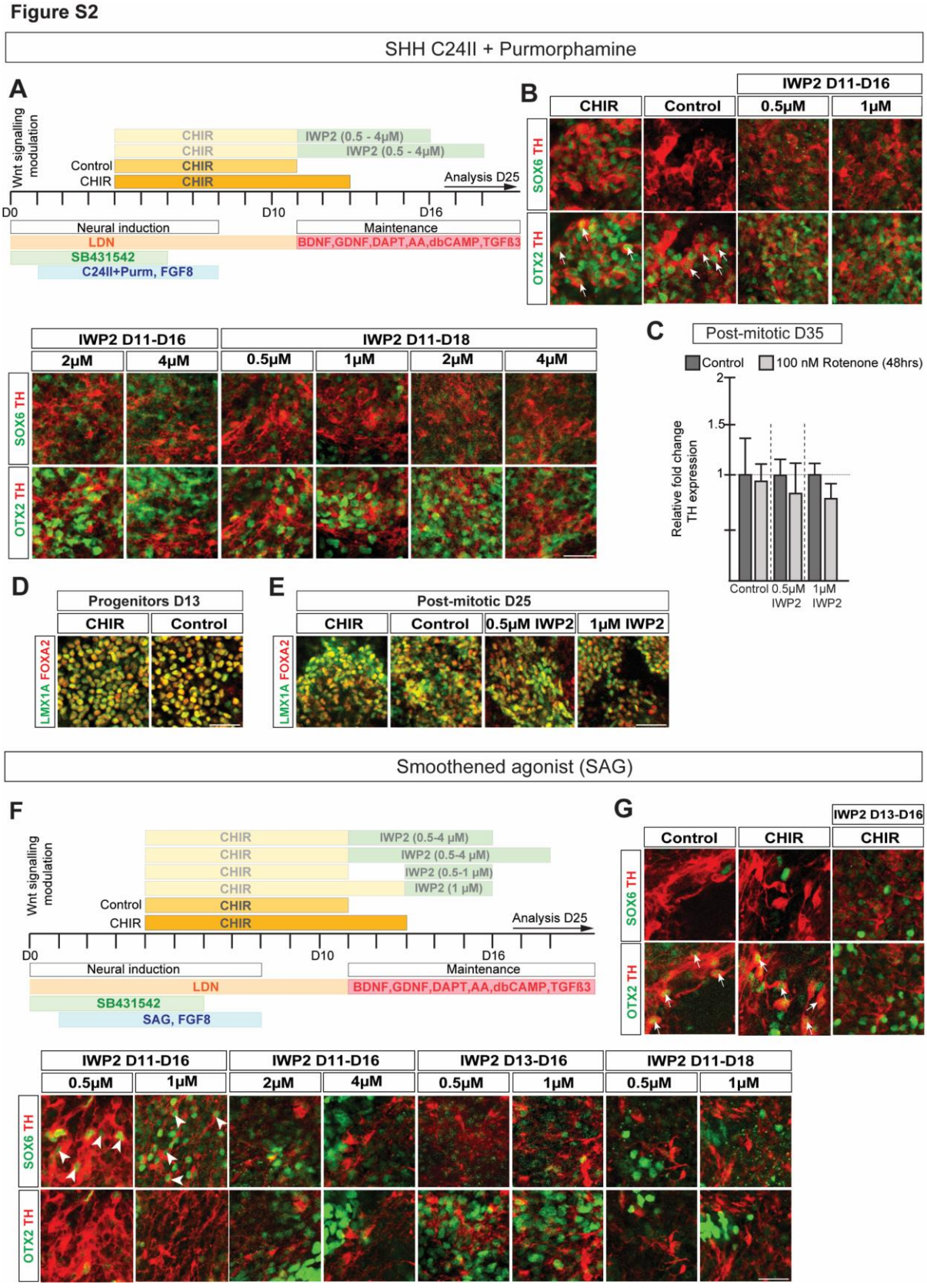

Figure S2 related to Figure 4. Timing and concentration of IWP2 addition and SHH signalling levels are critical for the efficient induction of SOX6. (A) Schematic

summary of hES cell differentiation protocol using SHH C24II+purmorphamine during progenitor specification. Conditions: CHIR (CHIR from d4-d13), control (CHIR from d4-d11) and IWP2 (IWP2 from day 11 following CHIR). **(B)** Combinatorial expression analysis of SOX6, OTX2 and TH by immunohistochemistry in SHH C24II+purmorphamine differentiated post-mitotic neurons (d25) following IWP2 treatment. Arrows point to OTX2 expressing TH labelled neurons. **(C)** qPCR analysis of *TH* levels in human ES cell derived DA cultures differentiated as described in **A** after treatment with 100nM rotenone for 48 hrs at d35 (n=3 independent experiments). Mean values ± SD; paired ttest. (**D, E**) Immunohistochemical analysis showing LMX1A and FOXA2 coexpression in progenitors (D13) and post-mitotic DA neurons (D25) after IWP2 (0.5μM and 1μM) exposure. **(F)** Schematic summary of hES cell differentiation protocol using Smoothened agonist (SAG) during progenitor specification. Diagram shows the timing of CHIR and IWP2 addition. Conditions: CHIR (CHIR from d4-d13), control (CHIR from d4-d11), IWP2 (IWP2 from d11 or d13 following CHIR). **(G)** Combinatorial expression analysis using antibodies against SOX6, OTX2 and TH reveals that SOX6 expression increases and OTX2 expression is reduced at D25 following IWP2 treatment when progenitors were differentiated in the presence of SAG. Arrows point to OTX2 expressing TH labelled neurons, while arrowheads indicate SOX6 expressing TH labelled neurons. See **F** for the different conditions that were tested. Note that the optimal IWP2 concentration range is between 0.5 and 1 μM added between d11 and d16. Scale bar: 50 μM.

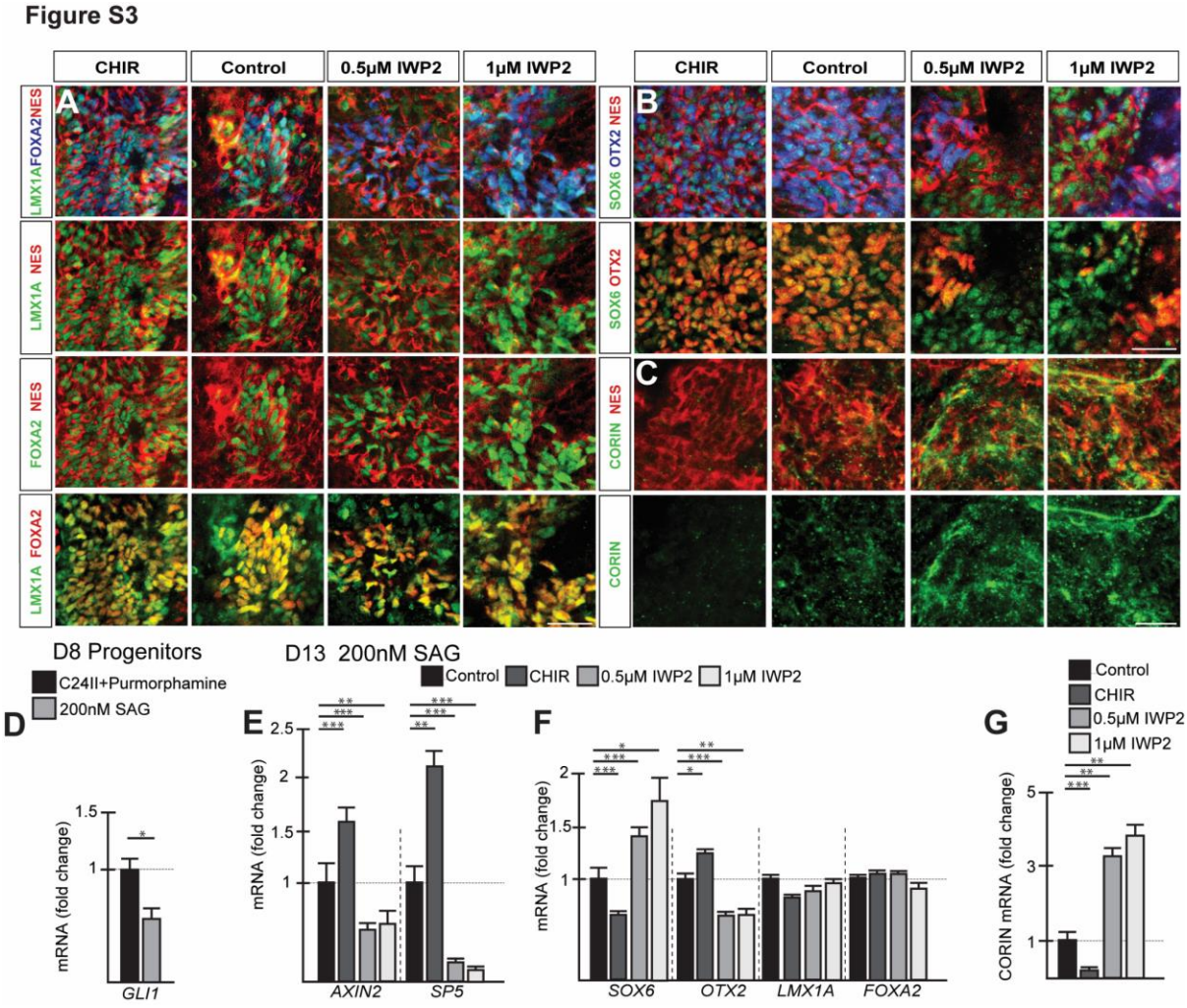

Figure S3 related to Figure 4. Maintenance of DA progenitor identity in IWP2 treated hES cell derived cultures differentiated in presence of SAG. (**A-G)** IWP2 was added from d11-d16 as described in **Fig. S4F**. **(A)** Immunohistochemical analysis showing that coexpression of LMX1A and FOXA2 is maintained in NESTIN^{+} progenitors when exposed to IWP2. **(B)** Immunohistochemical analysis of SOX6, OTX2 and NESTIN reveals patches of NESTIN^{+}/SOX6^{+}/OTX2^{-} progenitors in IWP2 treated cultures. **(C)** Representative images of CORIN and NESTIN immunolabelled progenitors. Note the increase in CORIN expression upon IWP2 treatment. **(D)** Comparison of *GLI1* mRNA levels in D8 progenitors differentiated either in presence of SHH C24II+purmorphamine or SAG. Expression levels were determined by qPCR. Mean values ± SD; unpaired ttest; n=3 independent experiments. **(E)** qPCR analysis of *AXIN2* and *SP5* expression in DA

progenitors (D13) treated with CHIR or IWP2. Gene expression in each condition is normalised to control. Mean values ± SD.; one-way ANOVA with Bonferroni correction; n=3 independent experiments. (**F, G**) qPCR analysis of *SOX6*, *OTX2*, *LMX1A*, *FOXA2* (**F**) and *CORIN* (**G**) expression in hESC derived DA progenitors (D13). Gene expression in each condition is normalised to the control. Mean values ± SD; one-way ANOVA with Bonferroni correction; n=3 independent experiments. *p < 0.05, **p < 0.01, ***p < 0.001. Scale bar: 50 μM.

Figure S4

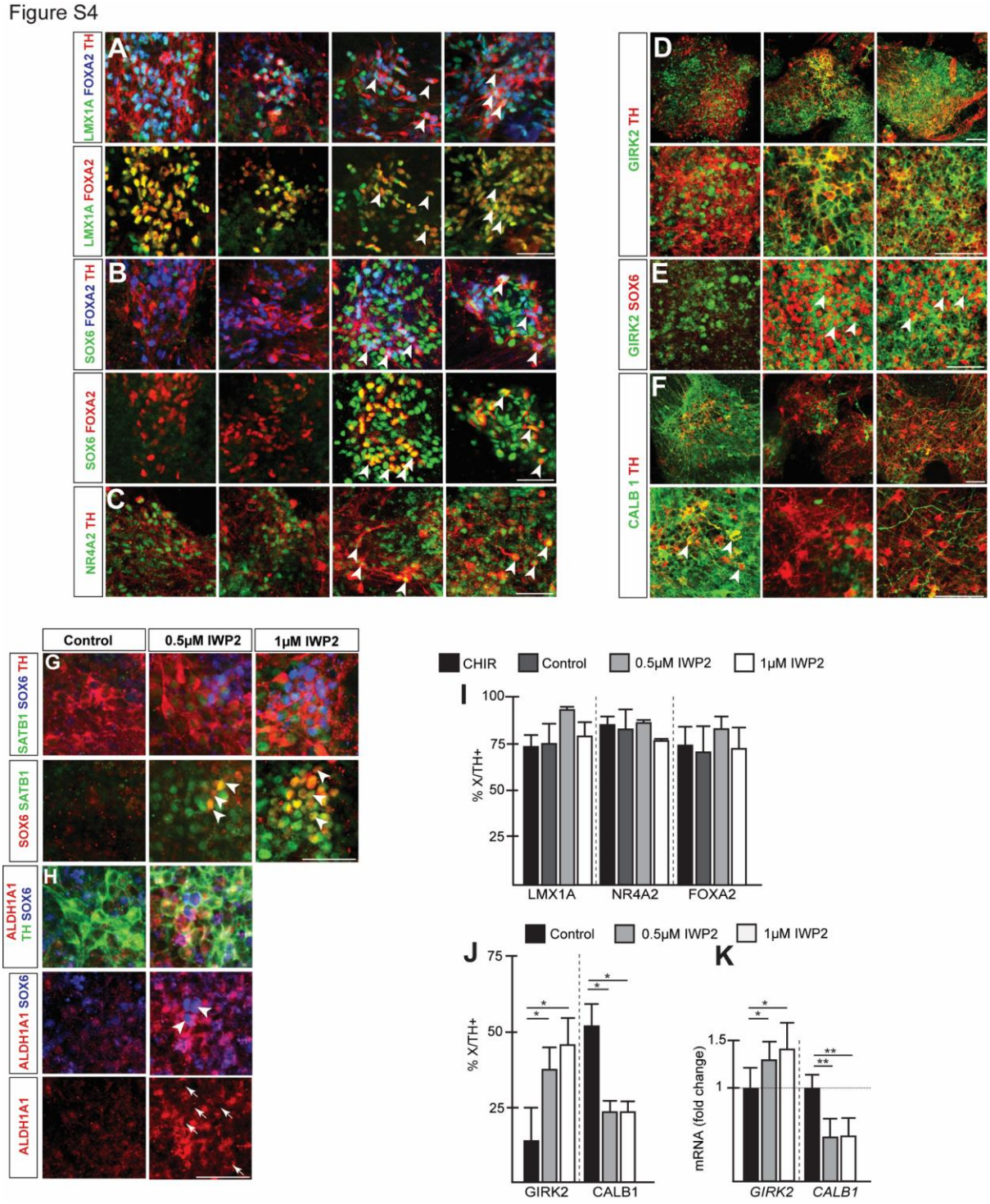

Figure S4 related to Figure 4. Maintenance of midbrain DA neuronal identity in IWP2 treated hES cell derived cultures differentiated in presence of SAG. (**A-K)** IWP2 was added from d11-d16 as described in **Fig. S2F**. **(A)** Immunohistochemistry reveals that midbrain DA markers LMX1A and FOXA2 are maintained in TH⁺ hESC derived post-mitotic neurons (d25) following IWP2 exposure. Arrowheads point to

$TH^+/LMX1A^+/FOXA2^+$neurons. **(B)** Immunohistochemistry shows that IWP2 induced $SOX6^+$ post-mitotic TH^+ neurons express FOXA2. Arrowheads point to $TH^+/SOX6^+/FOXA2^+$ neurons. **(C)** Midbrain DA marker NR4A2 is expressed in $TH^+/FOXA2^+$ post-mitotic neurons differentiated in presence of IWP2. Arrowheads indicate TH^+ neurons coexpressing NR4A2 and FOXA2. **(D, E)** Immunohistochemical analysis shows that GIRK2 expression is induced in $TH^+/SOX6^+$ hESC derived post-mitotic neurons (day 35) after IWP2 exposure. Arrowheads in **D** indicate overlap between GIRK2 and SOX6. **(F)** Immunohistochemical analysis shows that CALB1 expression decreases in hESC derived post-mitotic neurons (day 35) after IWP2 exposure. **(G)** Immunohistochemistry shows that SATB1 is expressed in $SOX6^+TH^+$ neurons (d35) differentiated in presence of IWP2. Arrowheads indicate coexpression of SOX6 and SATB1. **(H)** Immunohistochemical analysis shows coexpression of SOX6 and ALDH1A1 in TH+ neurons following exposure to IWP2 at day 35. Arrowheads point to ALDH1A1+/SOX6+ neurons and arrows point to nuclei of ALDH1A1 labelled neurons. **(I)** Percentage of TH^+ neurons expressing LMX1A, NR4A2 or FOXA2 differentiated in control, CHIR and IWP2 treated cultures (D25). Mean values ± SD; n=3 independent experiments. **(J)** Percentage of TH^+ neurons at day 35 expressing GIRK2 and CALB1 differentiated in absence (control) or presence of IWP2. Mean values ± SD; one-way ANOVA with Bonferroni correction; n=3 independent experiments. **(K)** qPCR analysis of *GIRK2* and *CALB1* mRNA levels from differentiated DA neurons (D35) after treatment with IWP2 in comparison to control cultures. Mean values ± SD; one-way ANOVA with Bonferroni correction; n=6 independent experiments. $^*p < 0.05$ and $^{**}p < 0.01$. Scale bar: 50 μM.

Figure S5

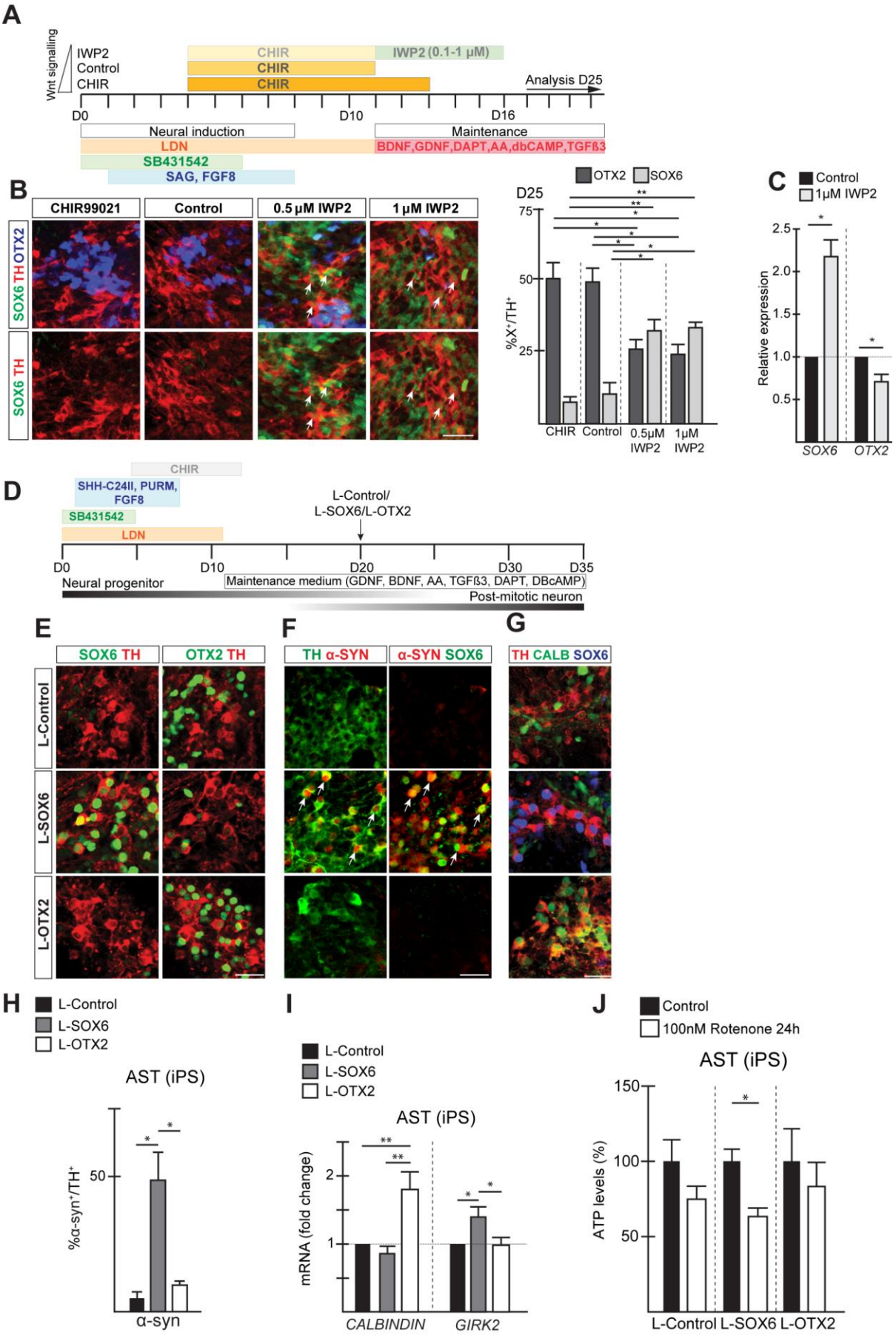
A
Wnt signalling
IWP2
Control
CHIR
CHIR
CHIR
IWP2 (0.1-1 µM)
Analysis D25
D0
D10
D16
Neural induction
Maintenance
LDN
BDNF,GDNF,DAPT,AA,dbCAMP,TGFß3
SB431542
SAG, FGF8
B
CHIR99021
Control
0.5 µM IWP2
1 µM IWP2
SOX6 TH OTX2
SOX6 TH
OTX2 SOX6
D25
%X+/TH+
CHIR
Control
0.5µM IWP2
1µM IWP2
C
Control
1µM IWP2
Relative expression
SOX6
OTX2
D
CHIR
SHH-C24II, PURM, FGF8
SB431542
LDN
L-Control/
L-SOX6/L-OTX2
D0
D10
D20
D30
D35
Neural progenitor
Maintenance medium (GDNF, BDNF, AA, TGFß3, DAPT, DBcAMP)
Post-mitotic neuron
E
SOX6 TH
OTX2 TH
L-Control
L-SOX6
L-OTX2
F
TH α-SYN
α-SYN SOX6
G
TH CALB SOX6
H
L-Control
L-SOX6
L-OTX2
AST (iPS)
%α-syn+/TH+
α-syn
I
L-Control
L-SOX6
L-OTX2
AST (iPS)
mRNA (fold change)
CALBINDIN
GIRK2
J
Control
100nM Rotenone 24h
AST (iPS)
ATP levels (%)
L-Control L-SOX6 L-OTX2

Figure S5 related to Figure 4 and 5. Reproducibility of methodology in AST iPS cell line. (A) Schematic summary of iPS cell differentiation protocol using Smoothened agonist (SAG) during progenitor specification. Conditions: CHIR (CHIR from d4-d13), control (CHIR from d4-d11) and IWP2 (IWP2 from day 11 following CHIR). **(B)** Immunohistochemistry showing SOX6 and OTX2 expression in TH^+ iPSCs derived post-mitotic neurons (day 25) following exposure to CHIR or IWP2. Arrows indicate $SOX6^+/OTX2^-$ TH labelled neurons in IWP2 treated cultures. Graph displays percentage SOX6 and OTX2 expressing TH labelled neurons under various culture conditions (n=3 independent experiments). mean values ± SD; one-way ANOVA with Bonferroni correction. **(C)** qPCR analysis of *SOX6* and *OTX2* mRNA levels in iPSCs derived DA neurons (D25) treated with 1μM IWP2 (n=4 independent experiments); mean values ± SD; paired ttest. **(D)** Schematic overview of differentiation conditions according to the floor plate protocol. Arrow indicates time point of lentiviral transduction. **(E)** Immunohistochemical analysis of SOX6 and OTX2 in virus transduced iPSCs derived cultures at d35, showing efficient transduction and expression the transcription factors. **(F)** Immunohistochemical analysis of α-SYN and SOX6 in virus transduced iPS cell derived cultures. Arrows point to α-SYN expression in TH^+/ $SOX6^+$ neurons. **(G)** Immunohistochemical analysis of CALB1 and SOX6 in virus transduced iPSCs derived cultures at d35, showing increased CALB1 expression in OTX2 but not in SOX6 transduced neurons. **(H)** Percentages of TH^+ neurons expressing α-SYN in virus transduced iPSCs derived cultures at d35 (n=3 independent experiments); mean values ± SD; one-way ANOVA with Bonferroni correction. **(I)** qPCR analysis of *CALB* and *GIRK2* mRNA levels in virus transduced iPSCs derived post-mitotic neurons (d35) (n=6 independent experiments); mean values ± SD; one-way ANOVA with Bonferroni correction. **(J)** Graph showing relative ATP levels in virus transduced iPSCs derived post-

mitotic neurons (D35) after treatment with DMSO (Control) or Rotenone (100nM, 24 hrs) (n=3 independent experiments); mean values ± SD; paired ttest. *p<0.05 and **p < 0.01. Scale bar: 50 µM.

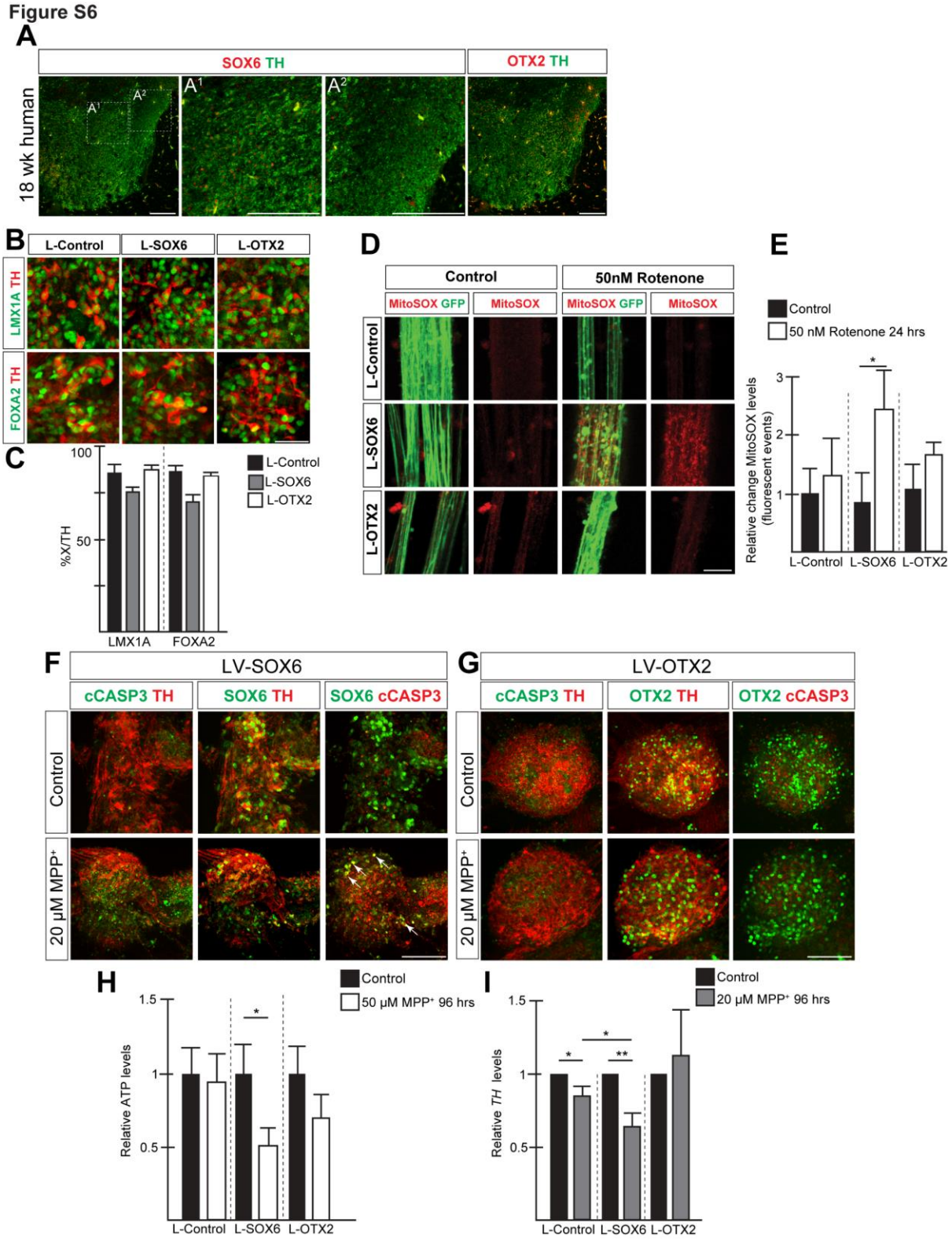

Figure S6 related to Figure 4, 5 and 6. Increased sensitivity to mitochondrial toxins in L-SOX6 transduced hES cell dopaminergic cultures. (A) Expression of SOX6 and OTX2 in human VTA dopaminergic neurons. A^1 and A^2 are higher magnified images of indicated regions. **(B)** LMX1A and FOXA2 expression in TH labelled DA neurons from human ES cell derived cultures (d35) transduced with indicated lentiviruses. **(C)** Percentages of LMX1A and FOXA2 expressing TH neurons after lentiviral transduction. Human ES cell derived cultures of d35. Values are shown as mean ± SD, n=3 independent experiments. **(D, E)** MitoSox analysis of virus transduced cultures treated at D35 with either DMSO or Rotenone for 24 hrs. **(D)** Live imaging of GFP and MitoSox in virus transduced cultures treated with either DMSO or Rotenone for 24 hrs at d35. All cultures were transduced with the lentivirus expressing GFP which enables to visualize the axons. **(E)** Relative fluorescence intensity MitoSox determined by flow cytometry. All values were normalized to untreated cultures transduced with control virus. Values represents the mean ± SD and significance was determined using the paired ttest; n=3 independent experiments. (**F**) Immunofluoresence marker analysis of L-SOX6 transduced cultures treated with MPP^+ at d35 for 96 hrs. Arrows point to cCASP3 and SOX6 double labelled cells only observed in MPP^+ treated cultures. **(G)** Immunofluoresence marker analysis of L-SOX6 transduced cultures treated with MPP^+ at d35 for 96 hrs. **(H)** Graph displays relative ATP levels of control and MPP^+ (d35, 96 hrs) treated virus transduced cultures. Values are shown as mean ± SD and significance was determined using the paired ttest; n=4 independent experiments. **(I)** Relative *TH* mRNA levels determined by qPCR. Values are shown as mean ± SD; one-way ANOVA with Bonferroni correction; n=6 independent experiments. *$p<0.05$ and **$p<0.01$. Scale bar: 50 µM (B, D, F, G), 200 µM (A).

Figure S7

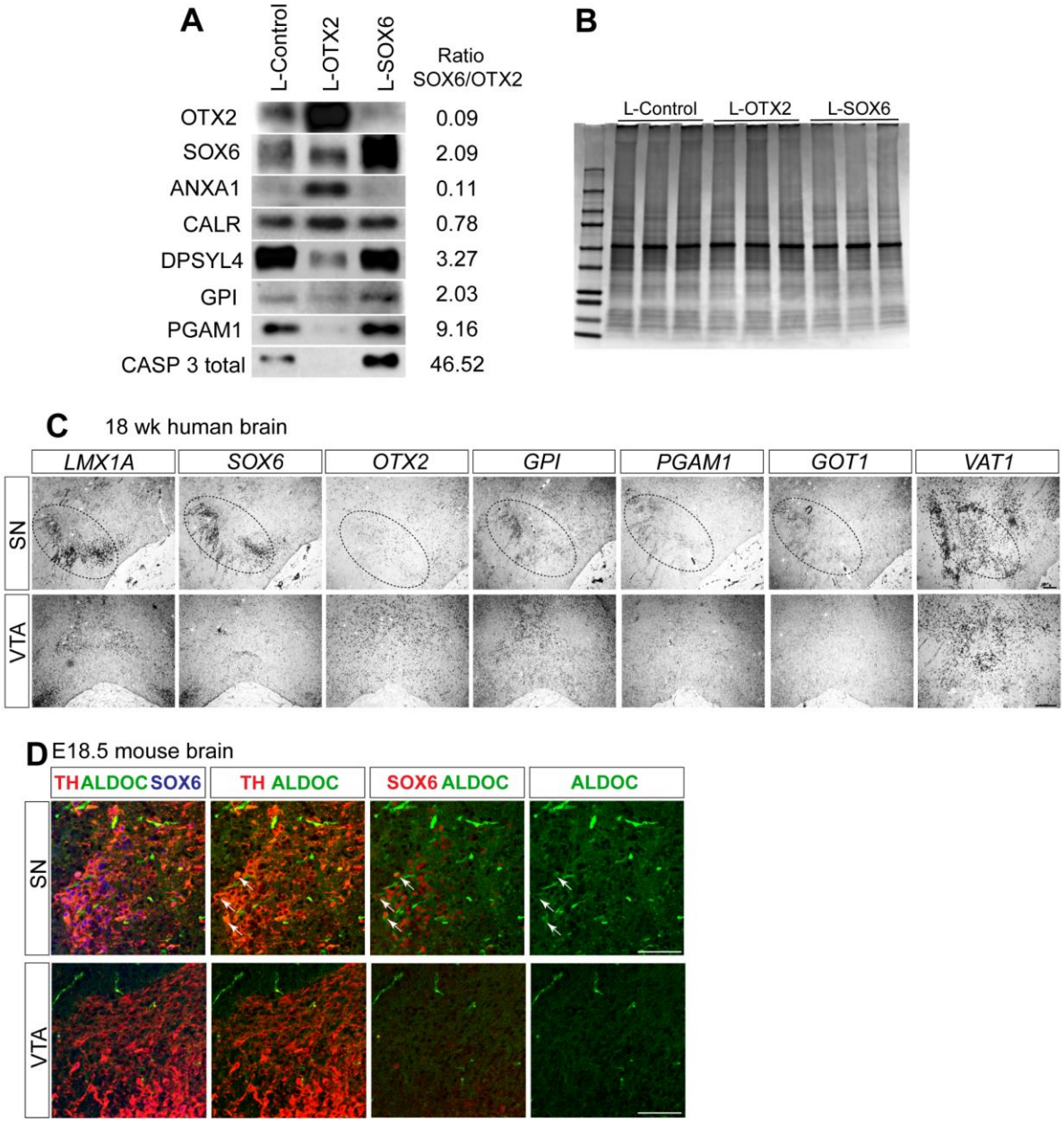

Figure S7 related to Figure 7. Verification of identified differential expressed proteins. (A) Western blot analysis show that proteins are expressed as predicted by the Mass-Spec analysis. **(B)** Coomassie Blue analysis that equal proteins quantities were used as an input. **(C)** Analysis of genes involved in metabolism in human foetal midbrain by in situ hybridization. Dashed circle indicate localization of the SN. **(D)** Immunohistochemical analysis of ALDOC and SOX6 expression in SN and VTA of E18.5

mouse brain. Arrows indicate overlap between ALDOC, Sox6 and TH. Scale bar: 100 µM (D), 200 µM (C).

Table S1

	Stage II	Stage III		Stage IV		Analysis stage V	
	EB	**Conditions**	**N days**	**Conditions**	**N days**	**%Sox6/TH ± SD**	**%Otx2/TH ± SD**
1	KSR	No growth factors	6	SHH,FGF8,	4	8.7 ± 6.7	86.9 ± 4.5
2	KSR	SHH,FGF8,	4	SHH,FGF8,	2	83.1 ± 5.9***	11.8 ± 6.80***
3	FBS	No growth factors	6	SHH,FGF8,	4	8.5 ± 2.9ns	86.0 ± 12.1ns
4	FBS	SHH,FGF8,	4	SHH,FGF8,	2	8.6 ± 9.7ns	85.2 ± 12.5ns
5	KSR	SHH,FGF8,	6	SHH,FGF8,	4	12.0 ± 2.0ns	82.7 ± 3.9ns
6[1]	KSR	No growth factors	4	SHH,FGF8,	2	79.0 ± 11.5	7.6 ± 4.6
7	KSR	SHH,FGF8,	4	SHH,FGF8,	4	18.1 ± 8.6	47.3 ± 19.9
8[1]	KSR	SHH,FGF8,	2	SHH,FGF8,	2	91.0 ± 0.4	4.5 ± 0.9
9	FBS	No growth factors	4	SHH,FGF8,	2	53.0 ± 3.2	20.2 ± 0.8
10	KSR	No growth factors	6	SHH, FGF8	2	47.3 ± 4.6	33.7 ± 6.7

Table S1 related to figure 1 and figure S1. Overview of the experimental outcomes of the several variants of the 5-stage protocol. Data shows average Sox6 and Otx2 labelled

TH positive neurons. Values are shown as mean ± SD from independent experiments. Protocols 1-5 (n=3) and protocols 6-10 (n=2). Unpaired ttest for protocols 2-5 in comparison to protocol 1. $^{***}p<0.001$; NS=not significant. [1]Note that reduced and deficiently developed TH^+ neurons were obtained when differentiated according to protocols 6 and 8 (see figure S1G).

Supplemental experimental procedures

Supplemental experimental procedures

5-stage protocol(Lee et al., 2000) : At the start of the differentiation (stage II) mES cells were separated from MEF cells by plating them on gelatinized tissue culture dishes for 45 minutes. Non-adherent cells were subsequently plated on bacterial dishes for 3 days in medium without LIF in presence of either 10% FBS or KSR. EBs were plated on gelatinized tissue culture dishes (Corning) and allowed to attach. Next day, medium was changed to DMEM/F12 (Gibco) supplemented with insulin (Gibco), apo-transferrin, sodium-selenite and fibronectin (all Sigma) (ITSFn medium; stage III). After 6 days neural precursor cells were splitted with TryplE Express and plated on poly-ornithine and laminin (Sigma) coated 24 well plates containing N3 medium, composed of DMEM/F12, insulin, apo-transferrin, sodium-selenite, progesterone, putrescine and laminin (all Sigma) plus 10 ng/ml bFGF (R&D), 100ng/ml FGF8 (R&D) and 100nM Smoothened agonist (SAG1.3, Calbiochem) (Stage IV). After 4 days neuronal differentiation was initiated by removal of the growth factors and addition of L-ascorbic acid (200 μM, Sigma) (stage V) (See table S1 – Protocol 1 and 3). After 6 days at stage V the medium was further supplemented with BDNF (10 ng/ml) and GDNF (10 ng/ml).

Medial Floorplate protocol: For EB formation the cells were plated in EB medium containing 10% KSR (stage II). After attachment of the EBs medium was changed the next day to N3 medium, plus 10 ng/ml bFGF, 100ng/ml FGF8 and 100nM SAG1.3 (stage III). After 4 days in stage III neural precursor cells were splitted with TryplE Express and plated on poly-ornithine and laminin coated 24 well plates containing N3 medium plus 10 ng/ml bFGF, 100ng/ml FGF8 and 100nM Hedgehog agonist Hh-Ag1.3 (Stage IV). After 2 days growth factors were removed and L-ascorbic acid (200 μM, Sigma) was added

(stage V) (See table S1 – Protocol 2). After 6 days in stage V medium was further supplemented with BDNF (10 ng/ml) and GDNF (10 ng/ml).

Other tested variations of the 5-stage (protocol 4-10): For EB formation either 10% FBS or KSR was added to the medium for 3 days (stage II). After attachment EB medium was changed the next day either to ITSFn, N3 medium or N3 medium plus 10 ng/ml bFGF, 100ng/ml FGF8 and 100nM SAG1.3 (stage III). Cells were kept at stage II between 2-6 days. Then neural precursor cells splitted and plated on poly-ornithine and laminin coated 24 well plates containing N3 medium plus 10 ng/ml bFGF, 100ng/ml FGF8 and 100nM SAG1.3 (Stage IV). After 2-4 days medium was changed to N3 medium containing L-ascorbic acid (200 μM, Sigma) (stage V) and cultured further as described before.

Wnt signalling modulation: 5-stage protocol derived cultures were exposed to 1 μM, 1.5 μM, 2 μM IWP2 or 5 μM IWR1, between days 9-15 (stage IV and V) of differentiation. Medial floorplate derived cultures were exposed to 2 μM CHIR between days 5-11 (stage III, IV and V) of differentiation.

Toxin exposure: For treatment with mitochondrial toxins MPP^+ (20 μM) or rotenone (50 nM) were added to the cultures after 12 days in stage V for 48 hrs. Ascorbic acid, BDNF and GDNF were removed from the cultures and DMSO treated cells served as a control. Meclizine (5 μM) was added alone or together with rotenone to the cultures for 48 hrs.

Maintenance and differentiation of hES and iPS cells

Maintenance: Human ES cells H9 (WA09, passage 32-48)(Thomson et al., 1998) and iPS cells AST23 (Edi001-A ECACC cat. no. 66540058, passage 25-35)(Devine et al., 2011) were cultured on Geltrex™ (Gibco) coated 6-well plates in Essential 8 medium (Gibco)(Chen et al., 2011) as described by the manufacturer's protocol. Cultures were passaged with 0.5 mM EDTA (Gibco) every 3 days in a 1:6 ratio. Medium was changed

daily. For maintenance of iPS cells 10 µM of Rock inhibitor (Tocris) was added to the medium after the split.

Differentiation of hES and iPS cells according to the floor plate protocol: Human ES and iPS cells were differentiated according to the floor plate protocol(Kriks et al., 2011) with the following modifications: Cells from a confluent well of 6 well plate were transferred to a well of a geltrex coated 24 well plate using EDTA and cultured overnight in Essential 8 medium. The next day neural induction was initiated by replacing the Essential 8 medium with a 1:1 mixture of N2 and B27 containing medium(Shi et al., 2012) supplemented with 100 nM LDN193189 (StemMacs) and 10 µM SB431542 (Tocris). On day 8 progenitors were dissociated with dispase (Life Technologies)(Shi et al., 2012) and cultured in a 24 well plate (1:2 ratio) in the presence of LDN and CHIR. The following concentrations of growth factors were added at a specific time point as previously described(Kriks et al., 2011; see figure 4D and 5B): 100 ng/ml SHH-C24II (R&D), 2 µM Purmorphamine (Calbiochem), 100 ng/ml FGF8 (R&D) and 3 µM CHIR (Stemgent). At day 11 the medium (N2/B27 1:1 mixture) was supplemented with the following survival promoting factors: BDNF (R&D; 25 ng/ml), GDNF (R&D; 25 ng/ml), TGFβ3 (R&D; 1 ng/ml), ascorbic acid (Sigma; 200 µM), DAPT (Sigma; 10 µM), db-cAMP (Sigma; 500 µM) until maturation. CHIR was added from d11 to d13 as previously described (Kriks et al., 2011; see figure 4D and 5B). Between d18 and d20 of differentiation the cultures were split at a 2:3 ratio with Accutase (Millipore) using the manufacturer's protocol and plated on laminin (Sigma), fibronectin (Sigma) and poly-L-ornithine (Sigma) coated plates(Kriks et al., 2011). The medium was changed on a daily basis.

Lentiviral constructs and transduction: cDNAs encoding human *Sox6*, human *Otx2* and GFP (Source Bioscience) were cloned into the lentiviral vector pRRL SIN.cPPT.PGK-GFP.WPRE (Addgene), with a PGK promoter driving transgene expression. The lentiviral

vector without insertion was used as a control. Lentiviral particles were produced in human embryonic kidney cells 293FT cells (Invitrogen) as described before(Panman et al., 2011). Human ES and iPS cell derived cultures were transduced with the virus (MOI=10) the day after the accutase split (between d18 and d20). The next day extra medium was added to the transduced wells and after 48 hrs the virus containing medium was removed and further cultured as described above. Cells were either analysed at d35 or exposed to indicated compounds.

Wnt signalling inhibition: Neural induction was initiated according to the floor plate protocol as described before(Kriks et al., 2011). Progenitors were exposed to either SHH C24II+Purmorphamine or smoothened agonist SAG (Calbiochem; 200nM) and were split at d8 with dispase. Wnt signalling inhibitors were added to specified dopaminergic progenitors at various concentrations (0.5μM, 1μM, 2μM and 4μM) of IWP2 or DKK1 (100 ng/ml). The following time-points of IWP2 treatment were tested (CHIR was removed at d11): d11-d16; d11-d18; d12-d16; d13-d16. For the last time point we removed CHIR either at d11 or at d13 from the culture medium. DKK1 was added from d11 till d16. We referred to the following control conditions: CHIR (CHIR was added until day 13) and control (CHIR was added until day 11). Cultures were kept in maintenance medium till d25 or d35 without splitting.

Toxin exposure: Human ES and iPS cell derived cultures were exposed to various chemical compounds at day 35 for indicated period of time. During toxin exposure BDNF and GDNF were omitted from the culture medium. Lentiviral transduced cultures were exposed to rotenone (50nM and 100nM) for 24 hours and MPP^+ (20μM and 50μM) for 96 hours. To alter the glycolytic rate, neurons were exposed to 6PG (10μM) or Meclizine (0.5μM) alone or in combination with rotenone (50nM and 100nM) for 24 hours. Cultures

exposed to Wnt signalling inhibitors were exposed to rotenone (50nM and 100nM) for 48 hours and MPP^+ (50μM) for 96 hours at d35.

Immunohistochemistry

E11.5 embryos were fixed in 4% PFA for 1h, washed 3 times for 5 min with PBS and put in 30 % sucrose overnight. Tissue was embedded in OCT and sectioned using a cryostat. Sections were air dried for 30 min and frozen at -80 C. Immunohistochemistry in the sections was performed as described(Panman et al., 2014). PS cell derived cultures were fixed with 2% PFA for 20 minutes and immunohistochemistry was performed as described(Panman et al., 2014). Nuclei were visualized by Dapi (Sigma) staining. Stained tissue sections or cells were analysed using a confocal microscope (LSM 510 Meta, Zeiss) or an Axiovert 200M (Zeiss). The antibodies and concentrations are shown in the supplemental information.

Cell quantification

Quantification of cells was performed manually from images obtained at 25X magnification. Labelled cells were counted versus the total number of either progenitor, post-mitotic or $DAPI^+$ cells. Cells were counted from at least three different images from three independent experiments and a minimum number of 200 cells per experiment was counted. Measurement were taken from distinct samples. Statistical significance was calculated by two-tailed student's t-test.

RNA Extraction and quantitative real-time PCR

Total RNA was extracted using RNeasy micro kit (Qiagen) according to the manufacturers' protocols. Biological replicates were obtained from at least three independent experiments. The RNA quality was assessed using a Nanodrop 2000 spectrophotometer (Thermo Scientific) prior to amplification. cDNA was synthesized from total RNA via reverse transcription using the reverse transcriptase SuperScriptIII (Invitrogen) and OligodT as primer (Invitrogen). Real-time qPCR was performed on a QuantStudio 6 Flex system (Thermo Fisher) using Fast SYBR Green Mastermix (Thermo Fisher). Gene expression values were normalized against RPL19 and fold change was calculated using the $2^{-\Delta\Delta CT}$ method(Livak and Schmittgen, 2001). The primer sequences used are shown in the supplementary resource table. Measurement were taken from distinct samples. Significance was determined by the two-tailed student's t-test.

ATP assay

By following the manufacturer´s protocol, the CellTiter-Glo Luminescent cell viability assay (Promega) was used to determine the ATP content within lentiviral transduced neurons (control, sox6 and otx2) treated with rotenone and 6PG (see chemical exposure). Measurements were performed in a 96 well plate (Greiner bio-one) with the GloMax 96 microplate luminometer (Promega). Measurement were taken from distinct samples. Significance was determined by the two-tailed student's t-test.

Mitosox assay

After rotenone (50nM) treatment for 24 hours, mature lentiviral transduced (GFP, SOX6, OTX2 and control) dopaminergic neurons were incubated, as described in the

manufacturer's protocol, with MitoSOX red reagent (Invitrogen), in order to detect mitochondrial superoxide.

Subsequently, neurons were dissociated with Accutase, transferred to 0.5mL microtubes with HBSS/Ca/Mg buffer (Gibco) and centrifuged at 200g for 10 min. Finally, the pellet was resuspended in PBS (Gibco) and samples were measured by fluorescence activated cell sorting using the BD FACSCanto II Flow Cytometer. Measurement were taken from distinct samples. Significance was determined by the two-tailed student's t-test.

In-situ hybridisation

E11.5 wild-type mouse embryos and human embryonic midbrain (CS16 and CS20) were fixed in 4% paraformaldehyde for 2 hours, shaking. After fixation they were incubated in 30% sucrose overnight at 4˚C and subsequently embedded in OCT Compound (VWR). Cryosections (12µM) of mouse and human embryonic brain were made for in situ hybridization. The human in-situ probes AXIN2, LMX1A, SOX6, OTX2, WNT-1 and the mouse in-situ probes Lmx1a, Sox6, Dkk3, Rspo2, Corin were produced by *in vitro* transcription of the linearized plasmid containing the gene of interest. The other listed in-situ probes were made by PCR amplification as previously described(Mong et al., 2014). The in-situ hybridisations were performed following standard procedures(Mong et al., 2014).

Human tissue analysis

Human embryos were collected after elective routine abortions with consent given by the pregnant women and approval from the Regional Human Ethics Committee, Stockholm.

Human foetal tissue of Carnegie stage 16, 20- and 18-weeks post conception was obtained from the Institute of Child Health (ICH), University College London. Tissue was fixed for hrs respectively in 4% PFA at 4°C, incubated in 30% sucrose and mounted in tissue-tek. Cryosections of 12 µM for cs 16 and 20 embryos and 14 µM sections of foetal tissue were made. For immunohistochemical analysis antigen retrieval was performed by incubating the sections for 20 minutes at 98 °C in 10 mM citric acid pH 6.0. Sections were subsequently washed in PBS and blocked with 0.1% triton and 5% donkey serum for 1 hr and incubated with primary antibodies overnight at 4°C, washed with PBS and subsequently incubated with secondary antibodies for one hour at RT.

Mouse lines

We used C57/Bl6 animals to obtain wild-type mouse embryonic tissue. The Tcf/Lef::H2B-GFP reporter mouse line(Ferrer-Vaquer et al., 2010) was kept as heterozygous on a C57/Bl6 background. All animal experiments are performed in accordance to the guidelines and legislation as regulated under the Animals Scientific Procedures Act 1986 (ASPA) and were approved by the Animal Welfare and Ethical Review Body (AWERB) of the University of Leicester.

Western blot analysis

Protein concentration was determined using Bradford Reagent (Sigma) and 20 µg of protein were separated by SDS-PAGE on an 8-16% gel and transferred onto a nitrocellulose membrane. Membranes were blocked for 1 hour at RT in 5% low-fat milk in TBS plus 0.5% Tween-20 (TBS-T) and incubated overnight at 4 °C with the primary anti-body diluted in 5% low-fat milk in TBS-T. Membranes were washed in TBS-T and incubated with horseradish peroxidase conjugated secondary antibodies for 1h at RT.

Bands were detected by ECL detecting solution (GE Healthcare) and the intensity of the signal was quantified using the Gel Doc EZ Imager software (Bio-Rad, California, USA).

Quantitative Mass-Spectrometry analysis

Sample preparation: For each condition three independent biological replicated were obtained. Protein concentration was determined using Bradford Reagent (Sigma). Each sample was divided over 3 three lanes (40 µg protein/lane) and migrated on a 10% SDS-PAGE gel (50V, 30 minutes). The gel was stained with Coomassie blue and each lane was subsequently cut horizontally in 3 bands and in-gel digested with bovine trypsin (Roche)(Soleilhavoup et al., 2016). Resultant peptides were dried using the SpeedVac.

Nanoflow liquid chromatography tandem mass-spectrometry (NanoLC-MS/MS): All experiments were performed on a dual linear ion trap Fourier transform mass spectrometer (FT-MS) LTQ Orbitrap Velos (Thermo Fisher Scientific) coupled to an Ultimate® 3000 RSLC Ultra High-Pressure Liquid Chromatographer (Thermo Fisher Scientific). Five microliters of each peptide extract was loaded on trap column for desalting and separated using nano-column as previously described(Pini et al., 2016; Soleilhavoup et al., 2016).

Protein identification and validation: Raw data files were processed using Proteome Discoverer software (version 2.1; Thermo Fischer Scientific). Precursor mass range of 350 –5000 Da and signal to noise ratio of 1.5 were the criteria used for generation of peak lists. MS/MS ion searches were performed using Mascot search engine version 2.6 (Matrix Science) against the NCBI nr database (mammalia taxonomy, 2017). Used parameters for database searches were as previously described(Pini et al., 2016; Soleilhavoup et al., 2016). Mascot results from the target and decoy databases searches

were subjected to Scaffold software (version 4.8.9, Proteome Software) using the protein cluster analysis option (assemble proteins into clusters based on shared peptide evidence). Peptide identifications were accepted if they could be established at greater than 95.0% probability as specified by the Peptide Prophet algorithm. Protein identifications were accepted if they could be established at greater than 95.0% probability as specified by the Protein Prophet algorithm and if they contained at least two identified peptides. The abundance of identified proteins within each sample was estimated by calculating the Exponentially Modified Protein Abundance Index (EMPAI).The False Discovery Rate (FDR) was < 0.01 %.

Label-free protein quantification: For comparative analyses, we employed Scaffold Q+ software (version 4.8.4, Proteome Software) to apply two independent quantitative methods: 1) Spectral Counting (SC) which counts and compares the number of fragment spectra identifying peptides of a given protein. 2) Average Precursor Intensity (API), which measures and compares the mass spectrometric signal intensity of peptide precursor ions belonging to a particular protein. Quantification was performed using the "Weighed Spectra" method. Thus, numbers of Normalized Weighed Spectra (NWS) were tabulated using experiment wide protein clustering. The reproducibility linked directly to the nanoLC-MS methodology was evaluated by the coefficients of variance (CV) for the three conditions in triplicate (SOX1-2-3 or OTX 1-2-3 or control 1-2-3) considering 3 technical replicates for each peptide extract analyzed by nanoLC-MS/MS (at total 81 runs) (Supplemental Table S2). Significance between treatments and control was determined using statistical tests within Scaffold Q+ software; Student's t-test for SC and API quantification, where $p < 0.05$ was considered significant. Limits of an average normalized weighted spectra (NWS) of ≥5 and fold change/ratio of ≥2 were included to increase validity of any comparisons made.

Pathway analysis: For pathway analysis L-SOX6 and L-OTX2 transduced neuronal cultures were compared and differentially expressed proteins (t-test $p<0.05$; $fc>2$) of both cell types were analysed for enrichment of their corresponding genes associated with pathways using ToppGene Server(Chen et al., 2009b).

References:

Chen, J., Bardes, E.E., Aronow, B.J., and Jegga, A.G. (2009b). ToppGene Suite for gene list enrichment analysis and candidate gene prioritization. Nucleic Acids Res *37*, W305-311.

Chen, G., Gulbranson, D.R., Hou, Z., Bolin, J.M., Ruotti, V., Probasco, M.D., Smuga-Otto, K., Howden, S.E., Diol, N.R., Propson, N.E*., et al.* (2011). Chemically defined conditions for human iPSC derivation and culture. Nat Methods *8*, 424-429.

Ferrer-Vaquer, A., Piliszek, A., Tian, G., Aho, R.J., Dufort, D., and Hadjantonakis, A.K. (2010). A sensitive and bright single-cell resolution live imaging reporter of Wnt/ss-catenin signaling in the mouse. BMC Dev Biol *10*, 121.

Livak, K.J., and Schmittgen, T.D. (2001). Analysis of relative gene expression data using real-time quantitative PCR and the 2(-Delta Delta C(T)) Method. Methods *25*, 402-408.

Pini, T., Leahy, T., Soleilhavoup, C., Tsikis, G., Labas, V., Combes-Soia, L., Harichaux, G., Rickard, J.P., Druart, X., and de Graaf, S.P. (2016). Proteomic Investigation of Ram Spermatozoa and the Proteins Conferred by Seminal Plasma. J Proteome Res *15*, 3700-3711.

Shi, Y., Kirwan, P., and Livesey, F.J. (2012). Directed differentiation of human pluripotent stem cells to cerebral cortex neurons and neural networks. Nat Protoc *7*, 1836-1846.

Key resources table

Gene	Mouse qPCR primer sequences	
Axin2	GCTCACCCATTTACCCAGGAC	TTCCTGTCCCTCTGCTGACTG
Corin	CTGCTCATTTTGCCAAGACA	ACAGCCCCATTCATCAGAAC
Lmx1a	TGCCTGGAGATCACATGCAC	CATATGGGAGCCCAGGTCAC
Otx2	AGAATCCAGGGTGCAGGTATG	TGGAGAGCTCTTCTTCTTGGC
RPL19	GGTGACCTGGATGAGAAGGA	TTCAGCTTGTGGATGTGCTC
Sox6	GTGTTTGCCTCTTGATGTGCC	TGGATGTAGTGAGAGGCGGTC
TH	GCTGGAGGATGTGTCTCACTTCT	CAGAAAATCACGGGCAGACAGTA

Gene	Human qPCR primer sequences	
AXIN2	ACAACAGCATTGTCTCCAAGCAGC	GCGCCTGGTCAAACATGATGGAAT
CALB1	CACAGCCTCACAGTTTTTCG	CCTTTCCTTCCAGGTAACCA
CORIN	CATATCTCCATCGCCTCAGTTG	GGCAGGAGTCCATGACTGT
FOXA2	TGGGAGCGGTGAAGATGGAAGGGCAC	TCATGCCAGCGCCCACGTACGACGAC
GIRK2 (KCNJ6)	AGGAGATCATGATTGAGTGAAGC	GGCCATTGTTGCAGTTTCTT
GLI1	AAGCGTGAGCCTGAATCTGT	GATGTGCTCGCTGTTGATGT
LMX1a	CAGCCTCAGACTCAGGTAAAAGTG	TGAATGCTCGCCTCTGTTGA
OTX2	GGGTATGGACTTGCTGCAC	CCGAGTGAACGTCGTCCT
RPL19	TGAGACCAATGAAATCGCCAATGC	ATGGACCGTCACAGGCTTGC
SOX6	GCTTCTGGACTCAGCCCTTTA	(Rev) GGCCCTTTAGCCTTTGGTTA
SP5	TCGGACATAGGGACCCAGTT	(Rev) CTGACGGTGGGAACGGTTTA
TH	TCATCACCTGGTCACCAAGTT	(Rev) GGTCGCCGTGCCTGTACT

Primary antibodies

Antibodies	Species	Company + Identifier	Dilution
α-SYN	Mouse	BD Biosciences (610786) AB_398107	1:500
Aldh1a1	Rabbit	Sigma (HPA050139) AB_2681031	1:500
Aldoc1	Mouse	Santa Cruz (sc-271593)	1:1000
Annexin A1	Mouse	Santa Cruz (sc-12740) AB_2057007	WB 1:1000
CALBINDIN	Rabbit	Swant (CB38) AB_2721225	1:500
Calreticulin	Rabbit	Abcam (ab2907) AB_303402	WB 1:1000
cCASP-3	Rabbit	Cell Signaling (9579S) AB_10897512	1:500
cCASP-3	Rabbit	Cell Signaling (9664S) AB_2070042	WB 1:1000
CORIN	Rat	R&D Systems (MAB2209) AB_2082224	1:500
Dpsyl4 (CRMP3)	Rabbit	Abcam (ab133287) AB_11154751	WB 1:1000
ENGRAIL-1	Mouse	DSHB (4G11) AB_528219	1:20
FOXA2	Goat	R&D Systems(AF2400) AB_2294104	1:500
γ-SYN	Rabbit	Abcam (ab55424) AB_2193398	1:3000
GFP	Rabbit	Abcam (ab6556) AB_305564	1:1000
GIRK2 (KCNJ6)	Goat	Abcam (ab65096) AB_1139732	1:500
GPI	Mouse	Santa Cruz (sc-365066) AB_10841426	WB 1:1000
Glyco-DAT	Rat	Merck Millipore (MAB369) AB_2190413	1:500
LMX1a	Rabbit	Merck Millipore (AB10533) AB_10805970	1:1000
LMX1a	Guinea Pig	gift from Johan Ericson	1:10000
NESTIN	Mouse	BD Biosciences (611658) AB_399176	1:1000
NURR1	Rabbit	Santa Cruz (sc-990) AB_2298676	1:1000
OTX2	Goat	R&D Systems (AF1979) AB_2157172	1:500
PGAM1	Rabbit	Cell Signaling (12098S) AB_2736922	WB 1:1000
SATB1	Rabbit	Abcam (ab7004) AB_955479	1:250
SOX6	Guinea pig	gift from Jonas Muhr	1:1500
SOX6	Mouse	Santa Cruz (sc-393314) N/A	WB 1:1000 IH 1:500
SOX6	Rabbit	Atlas Antibodies (HPA001923) AB_1080065	1:1000
TH	Mouse	Merck Millipore (MAB318) AB_2201528	1:1000
TH	Rabbit	Pel-Freez (P40101-150) AB_2617184	1:500
TH	Sheep	Pel-Freez (P60101-150)	1:500

Secondary antibodies

Anti-Goat Alexa Fluor 488	Donkey	Invitrogen (A-11055)	1:500
Anti-Goat Alexa Fluor 555	Donkey	Invitrogen (A-21432)	1:500
Anti-Goat Alexa Fluor 647	Donkey	Invitrogen (A-21447)	1:500
Anti-Mouse Alexa Fluor 488	Donkey	Invitrogen (A-21202)	1:500
Anti-Mouse Alexa Fluor 555	Donkey	Invitrogen (A-31570)	1:500
Anti-Rabbit Alexa Fluor 488	Donkey	Invitrogen (A-21206)	1:500
Anti-Rabbit Alexa Fluor 555	Donkey	Invitrogen (A-31572)	1:500
Anti-Rat Alexa Fluor 488	Donkey	Invitrogen (A-21208)	1:500
Anti-Guinea pig Cy5	Donkey	Stratech (706-175-148-JIR)	1:800

Primers designed for in-situ hybridization probe synthesis

Gene	**Primer sequences**	
h*CORIN*	ATGGTGACGAGGACTGCAAG	TCACTCACCTAAGCAGCCTGA
h *VAT1*	TTGAACCGGTCAGGGATGTG	TTCCCAACTTCTCCCTTCGC
m *Wnt1*	ATGCGCCAAGAGTGCAAATG	CGCTATGAACCCTGGGACTG

Other reagents

Reagents	Supplier	Cat number
Non-adherent bacterial dishes	Thermo Fisher	101R20
100mm tissue culture dishes	Corning	3296
24 well plates (mouse)	Corning	3337
Nunc- 24 well plates (human)	Thermo scientific	142475
Nunc- 6 well plates (human)	Thermo scientific	140675
96 well plates (ATP assay)	Greiner bio-one	655095
Accutase	Millipore	SCR005
Ascorbic acid	Sigma	A4403-100MG
ATP assay (CellTiter-Glo Luminescent cell viability assay)	Promega	G7570
B27 supplement	Life technologies	17504-044
BDNF	R&D	248-BD-025
bFGF	R&D	233-FB
CHIR99021	Stemgent	04-0004-10
DAPI	Sigma	D9564
DAPT	Sigma	D5942-25MG
Dibutyril cAMP	Sigma	D0627-250MG
Dispase	Life technologies	17105041
Dimethyl sulfoxide (DMSO)	Sigma	D8418
DKK1	R&D	5439-DK-010
DMEM high glucose	Gibco	41965-039
DMEM/F12 Glutamax	Gibco	31331-028
DMEM/F12	Gibco	10565-018
DPBS -Ca -Mg	Gibco	14190-094
Essential 8	Gibco	A1517001
Fetal bovine serum (FBS)	Gibco	16141-079
FGF8	R&D	423-F8-01M
Fibronectin	Sigma	F0895

Geltrex	Gibco	A1413302
GDNF	R&D	212-GD-050
HBSS/Ca/Mg	Gibco	14025-050
Insulin	Gibco	12585-014
IWP2	Tocris	3533
IWR1	Tocris	3532
KnockOut Serum Replacement (KSR)	Gibco	10828028
Laminin	Sigma	L2020
LDH cell viability assay	Promega	G7890
LDN193189	StemMacs	130-103-925
L-Glutamine	Gibco	25030-024
L(+)-Ascorbic Acid	Sigma	A7631
LIF	Merck Millipore	ESG1107
Meclizine dihydrochloride	Tocris	4245
β-Mercaptoethanol	Sigma	M3148
MitoSOX	Invitrogen	M36008
MPP dihydrochloride hydrate	Sigma	M7068
N2 supplement	Gibco	17502-048
Neurobasal	Gibco	12348-017
Non-essential amino acids	Gibco	11140-050
Paraformaldehyde	Sigma	P6148
Penicillin-Streptomycin	Thermo Fisher	15140-122
Poly-L-ornithine	Sigma	P4957
Progesterone	Sigma	P6149
Purmorphamine	Calbiochem	540220-5
Putrescine dihydrochloride	Sigma	P5780
Rotenone	Sigma	R8875
SHH-C24II	R&D	1845-SH-500
SAG1.3	Calbiochem	566660
SB431542	Tocris	1614/10
Sodium selenite	Sigma	S9133
TGFβ3	R&D	243-B3-010

6PG (6-Phosphogluconic acid trisodium salt)	Sigma	P6888
TryplE Express	Gibco	12604-013
UltraPure EDTA, pH 8.0	Gibco	15575-020